Transient dynamics of a quantum dot embedded between two superconducting leads and a metallic reservoir

R. Taranko, T. Kwapiński, and T. Domański*
Institute of Physics, M. Curie Skłodowska University, 20-031 Lublin, Poland

(Received 12 December 2018; revised manuscript received 8 March 2019; published 11 April 2019)

We study time-dependent subgap properties of a quantum dot (QD) embedded between two superconductors and another metallic lead, solving the Heisenberg equations of motion by the Laplace transform technique subject to the initial conditions. Focusing on the response of the system induced by a sudden coupling of the QD to external reservoirs, we analyze the transient currents and their differential conductance. We also derive analytical expressions for measurable quantities and find that they oscillate in time with the frequency governed by the QD coupling to superconducting reservoirs. Such quantum oscillations are damped due to relaxation processes caused by the normal lead, whereas their period is controlled by the phase difference ϕ between the order parameters of superconducting leads (except the case $\phi = \pi$, when all observables evolve to their stationary values without any oscillations). We also explore time-dependent development of the subgap quasiparticles and find their signatures measurable in the differential conductance. We evaluate (numerically and analytically) three typical time scales, characterizing the initial and large-time stages of the transient dynamics which in the asymptotic limit ($t \to \infty$) drives these subgap quasiparticles to the true Andreev states.

DOI: 10.1103/PhysRevB.99.165419

I. INTRODUCTION

Transient effects of the quantum dot (QD) systems have been intensively studied over recent years, providing useful insight into the electron transport properties. These effects could be of special importance in experiments on nanoscopic devices, where different types of time-dependent pulses can effectively control the electron flow. Transient effects have been studied, both theoretically and experimentally, for the QDs coupled to the metallic (conducting) electrodes [1–67] and in the presence of superconducting reservoirs [68–84]. Numerous theoretical approaches have been developed to deal with such time-dependent problems, e.g., the iterative influence-functional path integral [35], Keldysh formalism and time-dependent partition-free approach [40], weak-coupling continuous-time Monte-Carlo method [27], and many other techniques [53,61].

The coherent oscillations and current beats have been found in a short-time response of a system upon abrupt change of the bias voltage [9,14]. From the periods of the current beats it is possible to estimate the values of the QDs energy levels or the hopping parameters between them [38,51,57]. The transient current characteristics can also be used to determine the spin relaxation time in some QD systems [4]. Such phenomena have been investigated for QDs coupled to the normal leads as a result of the bias voltage pulse [5,22,29,31,36,41,53,60,75], driven by an arbitrary time-dependent bias [26,27,40,53,61], by a sequence of rectangular pulses applied to the input lead [17,32] or applied to the contact gradually switched on in time [25]. The transient dynamics has also been studied for QD after a sudden symmetrical connection to the leads [27,37,78,85] or asymmetrically coupled to electrodes following a sudden change of the QD energy levels [11]. The transient heat generation driven by a steplike pulse bias within the Anderson-Holstein model or the time-dependent current through QD suddenly coupled to a vibrational mode have been studied in nanostructures with the normal [19,30,47,56,63] or superconducting electrodes [71].

Technological progress in the real-time detection of single electrons has opened a possibility for studying electron transport from a perspective of the stochastic processes. Among theoretical tools for investigating the electron hopping statistics there are, e.g., the full counting statistics (FCS) and the waiting time distribution (WTD) [54,55,62,66,73,79]. These theoretical techniques have been successfully applied to investigations of the transient processes via QD coupled to the normal leads [62] or in hybrid systems with superconductors [66,73,79]. Time-dependent processes are often investigated numerically, however, in exceptional cases some analytical results can give deeper insight into the considered problem. For instance, WTD in the normal lead-QD-superconducting junction exhibit the coherent oscillations between the empty and doubly occupied QD [73]. Similarly, some analytical calculations are possible for the energy transport in the polaronic regime described within the FCS method [59], for transient dynamics after a quench [64], for a phononic heat transport in the transient regime [65], or for transient heat generation under a steplike bias pulse [44].

In this paper we analyze the subgap transport properties of a system comprised of a single QD which is tunnel coupled to one metallic (normal) and two superconducting electrodes, focusing on transient effects driven by abrupt coupling of these constituents. It is natural that oscillations of the transient current would appear as a result of such quench, and they should depend on initial conditions of the system. Such hybrid nanostructures with QD between the normal and supercon-

*doman@kft.umcs.lublin.pl

ducting electrodes reveal many interesting effects with potential applications in nanoelectronics, spintronics, or quantum computing [29,30,42,63,64]. The superconducting reservoir affects the QD via proximity effect and could be responsible for the Cooper-pair tunneling and Josephson currents, even in the absence of any bias voltages. An additional normal electrode coupled to the system allows for good control of the electron transport [86–92] and could significantly affect the transient phenomena. Our goal is to investigate analytically the time-dependent QD occupation, the currents flowing from the normal and superconducting leads, the induced QD pairing, the conductance, and the time evolution of the Andreev bound states (ABS) [90,93–97]. The formation of ABS signifies that superconducting correlations are induced in the QD via the proximity effect. We investigate the appearance in time of these states and study their spin dependence. To perform analytical time-dependent calculations we assume that the superconducting gap of both superconducting leads is the largest energy scale and we put it equal to infinity. Nevertheless, the realistic physics in the Andreev transport regime is still captured in this limit. Knowledge of the analytical formulas allows us to find the answers to such questions as: (i) how do the considered quantities and their characteristics depend on the QD energy levels or the individual coupling of the QD with a given lead, (ii) what is the time period and frequency of these time-dependent quantities, and many related issues. Our investigations allow us also to analyze time evolution of the subgap quasiparticles and their dependence on the phase difference between the superconducting reservoirs. In our calculations we apply the equation of motion method for the second quantization operators and obtain their analytical form using the Laplace transform technique. Numerical calculations could provide results only for a specific choice of parameters and would not give deep insight into specific dependence of here considered quantities of our system. In this context the analytical calculations are much more general and could have some advantage over numerical data.

The paper is organized as follows. In Sec. II we present our model and discuss the theoretical formalism. The time-dependent QD occupancy is analyzed in Sec. III, whereas Sec. IV is devoted to the proximity-induced pairing effects. The normal and superconducting transient currents through the QD are analyzed in Sec. V and in Sec. VI we discuss the subgap conductance. In Sec. VII we briefly address the correlation effects and finally, in Sec. VIII, we summarize our study.

II. MODEL AND THEORETICAL DESCRIPTION

The system under consideration consists of a QD placed between two superconducting leads ($S1$ and $S2$) and one metallic electrode N, see Fig. 1.

The model Hamiltonian for this system can be written in the following form: $H = H_{S1} + H_{S2} + H_N + H_{QD} + H_{\rm int}$, where H_{Sj} ($j = 1, 2$) describes electrons in the left or right superconducting lead

$$H_{Sj} = \sum_{q\sigma} \varepsilon_{q_j,\sigma} c^+_{q_j\sigma} c_{q_j\sigma} + \sum_{q_j} \left(\Delta_j c^+_{-q_j\uparrow} c^+_{q_j\downarrow} + \text{H.c.}\right), \quad (1)$$

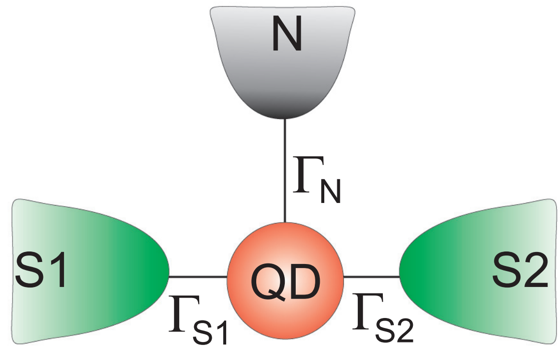

FIG. 1. Schematic diagram for a quantum dot coupled with two superconducting leads (S1 and S2) and one normal (metallic) electrode (N).

H_N refers to the normal lead, $H_N = \sum_{k\sigma} \varepsilon_{k\sigma} c^+_{k\sigma} c_{k\sigma}$, H_{QD} describes the QD, $H_{QD} = \sum_\sigma \varepsilon_\sigma c^+_\sigma c_\sigma$. Electron transitions between external leads and the QD are established by the tunnel Hamiltonian:

$$H_{\rm int} = \sum_{k,\sigma} V_{k\sigma} c^+_{k\sigma} c_\sigma + \sum_{j=1,2} \sum_{q\sigma} V_{q_j\sigma} c^+_{q_j\sigma} c_\sigma + \text{H.c.} \quad (2)$$

We assume that the electron dispersion in all leads is spin independent and impose the order parameters, Δ_j, of the superconducting leads to be phase dependent, $\Delta_j = |\Delta_j| \exp{(i\varphi_j)}$. In our notation k (q_j) shall denote itinerant states of the normal (superconducting) lead.

We are going to study time response of this system on abrupt switching of the coupling parameters. We shall thus calculate the time-dependent QD occupations, $n_\sigma(t)$, and the currents flowing from the leads, $j_{N\sigma}(t)$, $j_{S_j\sigma}(t)$. Additionally we will compute $\langle c_\downarrow(t) c_\uparrow(t)\rangle$, which corresponds to the electron pairing induced at QD via proximity effect. In what follows we assume that all couplings between the QD and the leads are suddenly switched on at $t = 0^+$ (for $t \leqslant 0$ the QD is decoupled from the leads). The time evolution of the considered quantities for $t > 0$ depends on the initial QD filling and the chemical potentials. As time goes to infinity, we reproduce the stationary limit results known for the corresponding system. In this paper we use the Laplace transform method and our strategy in the calculations is as follows: We construct the closed set of the equation of motion for creation and annihilation operators (in the Heisenberg representation) $c_\sigma(t)$, $c_{k\sigma}(t)$, $c_{q_j\sigma}(t)$, $c^+_\sigma(t)$, $c^+_{k\sigma}(t)$, $c^+_{q_j\sigma}(t)$, using the Laplace transformations for these differential equations we obtain the set of coupled algebraic forms $c(s) = \int_0^\infty dt e^{-st} c(t)$ for all considered operators. For instance, the QD occupation $n_\sigma(t)$ can be found from the relation

$$n_\sigma(t) = \langle \mathcal{L}^{-1}\{c^+_\sigma(s)\}(t) \cdot \mathcal{L}^{-1}\{c_\sigma(s)\}(t)\rangle, \quad (3)$$

where $\mathcal{L}^{-1}\{a(s)\}(t)$ stands for the inverse Laplace transform of $a(s)$ and $\langle ...\rangle$ is the quantum statistical averaging.

Let us find the Laplace transforms of operators $c_\sigma(t)$ and $c_{q_j\sigma}(t)$ which are required to calculate the QD occupancy $\langle c^\dagger_\sigma(t) c_\sigma(t)\rangle \equiv n_\sigma(t)$, the QD induced pairing $\langle c_\downarrow(t) c_\uparrow(t)\rangle$, and the currents flowing from the leads. We write the Laplace transformed equations of motions for the closed set of twelve operators (in the Heisenberg representation): $c_\uparrow$, $c^\dagger_\downarrow$, $c_{k\uparrow}$, $c^\dagger_{k\downarrow}$, $c_{q_j\uparrow}$, $c^\dagger_{-q_j\downarrow}$, $c^\dagger_{q_j\downarrow}$, $c_{-q_j\uparrow}$, $j=1,2$.

$$(s+i\varepsilon_\uparrow)c_\uparrow(s) = -i\sum_{r=k,q_1,q_2} V_r c_{r\uparrow}(s) + c_\uparrow(0), \tag{4a}$$

$$(s+i\varepsilon_{q_j})c_{q_j\uparrow}(s) = -iV_{q_j}c_\uparrow(s) - i\Delta_j c^\dagger_{-q_j\downarrow}(s) + c_{q_j\uparrow}(0), \tag{4b}$$

$$(s-i\varepsilon_{q_j})c^\dagger_{-q_j\downarrow}(s) = iV_{q_j}c^\dagger_\downarrow(s) - i\Delta^*_j c_{q_j\uparrow}(s) + c^\dagger_{-q_j\downarrow}(0), \tag{4c}$$

$$(s+i\varepsilon_k)c_{k\uparrow}(s) = -iV_k c_\uparrow(s) + c_{k\uparrow}(0), \tag{4d}$$

$$(s-i\varepsilon_\downarrow)c^\dagger_\downarrow(s) = i\sum_{r=k,q_1,q_2} V_r c^\dagger_{r\downarrow}(s) + c^\dagger_\downarrow(0), \tag{5a}$$

$$\big(s-i\varepsilon_{q_j}\big)c^\dagger_{q_j\downarrow}(s) = iV_{q_j}c^\dagger_\downarrow(s) - i\Delta^*_j c_{-q_j\uparrow}(s) + c^\dagger_{q_j\downarrow}(0), \tag{5b}$$

$$\big(s+i\varepsilon_{q_j}\big)c_{-q_j\uparrow}(s) = -iV_{q_j}c_\uparrow(s) - i\Delta_j c^\dagger_{q_j\downarrow}(s) + c_{-q_j\uparrow}(0), \tag{5c}$$

$$(s-i\varepsilon_k)c^\dagger_{k\downarrow}(s) = iV_k c^\dagger_\downarrow(s) + c^\dagger_{k\downarrow}(0). \tag{5d}$$

From Eqs. (4a)–(4d) and Eqs. (5a)–(5d) we get

$$c_\uparrow(s)M^{(+)}_\uparrow(s) = A(s) - iK(s)c^\dagger_\downarrow(s), \tag{6a}$$

$$c^\dagger_\downarrow(s)M^{(-)}_\downarrow(s) = B(s) - iK^*(s)c_\uparrow(s), \tag{6b}$$

where

$$K(s) = \sum_{j=1,2}\frac{V^2_{q_j}\Delta_j}{s^2+\varepsilon^2_{q_j}+|\Delta_j|^2}, \tag{7}$$

$$A(s) = -\sum_{j=1,2}\frac{V_{q_j}\big(\Delta_j c^+_{-q_j\downarrow}(0) + i\big(s-i\varepsilon_{q_j}\big)c_{q_j\uparrow}(0)\big)}{s^2+\varepsilon^2_{q_j}+|\Delta_j|^2} -i\sum_k \frac{V_k c_{k\uparrow}(0)}{s+i\varepsilon_k} + c_\uparrow(0), \tag{8}$$

$$B(s) = \sum_{j=1,2}\frac{V_{q_j}\big(\Delta^*_j c_{-q_j\uparrow}(0) + i\big(s+i\varepsilon_{q_j}\big)c^+_{qj\downarrow}(0)\big)}{s^2+\varepsilon^2_{q_j}+|\Delta_j|^2} + i\sum_k \frac{V_k c^+_{k\downarrow}(0)}{s-i\varepsilon_k} + c^+_\downarrow(0), \tag{9}$$

$$M^{(+/-)}_\sigma(s) = s \pm i\varepsilon_\sigma + \sum_{j=1,2}\frac{V^2_{q_j}\big(s\mp i\varepsilon_{q_j}\big)}{s^2+\varepsilon^2_{q_j}+|\Delta_j|^2} + \sum_k \frac{V^2_k}{s\pm i\varepsilon_k}. \tag{10}$$

Solving Eqs. (6a), (6b) we obtain for $c_\uparrow(s)$

$$c_\uparrow(s) = \frac{M^{(-)}_\downarrow(s)A(s) - iK(s)B(s)}{M^{(+)}_\uparrow(s)M^{(-)}_\downarrow(s) + K(s)K^*(s)}. \tag{11}$$

Repeating the same procedure to the set of operators: $c_\downarrow$, $c^\dagger_\uparrow$, $c^\dagger_{k\uparrow}$, $c_{k\downarrow}$, $c_{q_j\downarrow}$, $c^\dagger_{-q_j\uparrow}$, $c^\dagger_{q_j\uparrow}$, and $c^\dagger_{-q_j\downarrow}$ one can get

$$c_\downarrow(s) = \frac{M^{(-)}_\uparrow(\varepsilon)B^+(s) + iK(s)A^+(s)}{M^{(-)}_\uparrow(s)M^{(+)}_\downarrow(s) + K(s)K^*(s)}. \tag{12}$$

Laplace transforms of $c^\dagger_\uparrow$ and $c^\dagger_\downarrow$ can be obtained, taking the hermitian conjugation of $c_\uparrow$ and $c_\downarrow$, respectively.

In the wide-band limit approximation and for $|\Delta_j| = \infty$ the functions $M^{+/-}_\sigma(s)$ and $K(s)$ can be expressed in the following analytical forms: $M^{+/-}_\sigma(s) = s \pm i\varepsilon_\sigma + \Gamma_N/2$, and $K(s) = (\Gamma_{S_1}e^{i\varphi_1} + \Gamma_{S_2}e^{i\varphi_2})/2$. Here we have assumed $\Gamma_{N/S_j} = 2\pi\sum_{k/q_j} V^2_{k/q_j}\delta(\varepsilon-\varepsilon_{k/q_j})$ and $\varepsilon_{k\sigma} = \varepsilon_k$, $\varepsilon_{q_j\sigma} = \varepsilon_{q_j-\sigma} = \varepsilon_{-q_j}$. As an example, let us present the explicit form of the Laplace transform for $c_\uparrow(t)$

$$\begin{aligned} c_\uparrow(s) = \frac{1}{(s-s_3)(s-s_4)}\Bigg\{&\left(s - i\varepsilon_\downarrow + \frac{\Gamma_N}{2}\right)\\ &\times\Bigg[c_\uparrow(0) - i\sum_k \frac{V_k\, c_{k\uparrow}(0)}{s+i\varepsilon_k}\\ &- \sum_{j=1,2}\frac{iV_{q_j}\big(s-i\varepsilon_{q_j}\big)c_{q_j\uparrow}(0) + V_{q_j}\Delta_j c^\dagger_{-q_j\downarrow}(0)}{s^2+\varepsilon^2_{q_j}+|\Delta_j|^2}\Bigg]\\ &-\frac{i}{2}\big(\Gamma_{S1}e^{i\varphi_1} + \Gamma_{S2}e^{i\varphi_2}\big)\Bigg[c^\dagger_\downarrow(0) + i\sum_k \frac{V_k\, c^\dagger_{k\downarrow}(0)}{s-i\varepsilon_k}\\ &+ \sum_{j=1,2}\frac{iV_{q_j}\big(s+i\varepsilon_{q_j}\big)c^\dagger_{q_j\downarrow}(0) + V_{q_j}\Delta_j c_{-q_j\uparrow}(0)}{s^2+\varepsilon^2_{q_j}+|\Delta_j|^2}\Bigg]\Bigg\}, \end{aligned} \tag{13}$$

where $s_{3,4} = \frac{1}{2}[-i(\varepsilon_\uparrow - \varepsilon_\downarrow) - \Gamma_N \pm i\sqrt{\delta}]$, $\delta = (\varepsilon_\uparrow + \varepsilon_\downarrow)^2 + \Gamma_{12}$, and $\Gamma_{12} = \Gamma^2_{S_1} + \Gamma^2_{S_2} + 2\Gamma_{S_1}\Gamma_{S_2}\cos(\varphi_1 - \varphi_2)$.

Note that in the formula (13) there appears the finite superconducting energy gap Δ_j. The limit $|\Delta_j| = \infty$ will be imposed later on, when computing the expectation values of the product of two corresponding operators, e.g., $\langle c^\dagger_\sigma(t)c_\sigma(t)\rangle$ or $\langle c^\dagger_\sigma(t)c_{q_j\sigma}(t)\rangle$. Additionally, expression for $c_{q_j\sigma}(s)$ needed for calculations of the currents flowing between the QD and the superconducting leads can be obtained from Eqs. (4b), (4c), (11), (12) and it reads

$$\begin{aligned} c_{q_j\sigma}(s) = \frac{1}{s^2+\varepsilon^2_{q_j}+|\Delta_j|^2}\big[&\big(s-i\varepsilon_{q_j}\big)\big(c_{q_j\sigma}(0) - iV_{q_j}c_\sigma(s)\big)\\ &+\alpha V_{q_j}\Delta_j c^+_{-\sigma}(s) - i\alpha\Delta_j c^+_{-q_j-\sigma}(0)\big], \end{aligned} \tag{14}$$

where $\alpha = +(-)$ for $\sigma = \uparrow$ $(\downarrow)$. Using these formulas for $c_\sigma(s)$ and $c_{q_j\sigma}(s)$ we can analytically determine the QD occupancy, pairing parameter, subgap currents and its differential conductance.

In the following we set $e = \hbar = k_B \equiv 1$ and make use of the wide-band limit approximation. All numerical calculations shall be performed for $\Gamma_{S_1} = \Gamma_{S_2} = \Gamma_S$ and $\mu_N = 0$, unless stated otherwise. The energies, currents, and time are expressed in units of Γ_S, $e\Gamma_S/\hbar$, and $\hbar/\Gamma_S$, respectively. We assume the chemical potentials of superconducting leads $\mu_{S_1} = \mu_{S_2} = 0$ to be grounded. For experimentally available values of Γ_S, $\Gamma_S \sim 200$ μeV [82–84], the typical time and current units would be ∼3.3 psec and ∼48 nA, respectively.

III. QUANTUM DOT OCCUPANCY

Let us consider the time-dependent QD occupancy after abrupt coupling (at $t = 0^+$) to the normal and superconducting electrodes. We assume no bias voltage between electrodes and make use of the wide band limit approximation and impose $|\Delta_j| = \infty$. Under these assumptions the QD occupation, $n_\sigma(t)$, reads (cf. [80] for N-QD-S and [98] for N-QD-N systems):

$$
\begin{aligned}
n_\sigma(t) = {}& \mathcal{L}^{-1}\left\{\frac{s + i\varepsilon_{-\sigma} + \Gamma_N/2}{(s-s_1)(s-s_2)}\right\}(t)\mathcal{L}^{-1}\left\{\frac{s - i\varepsilon_{-\sigma} + \Gamma_N/2}{(s-s_3)(s-s_4)}\right\}(t)n_\sigma(0) \\
&+ \frac{\Gamma_{12}}{4}\mathcal{L}^{-1}\left\{\frac{1}{(s-s_1)(s-s_2)}\right\}(t)\mathcal{L}^{-1}\left\{\frac{1}{(s-s_3)(s-s_4)}\right\}(t)(1 - n_{-\sigma}(0)) \\
&+ \sum_{k_1,k_2} V_{k_1}V_{k_2}\mathcal{L}^{-1}\left\{\frac{s + i\varepsilon_{-\sigma} + \Gamma_N/2}{(s-s_1)(s-s_2)\left(s - i\varepsilon_{k_1}\right)}\right\}(t)\mathcal{L}^{-1}\left\{\frac{s - i\varepsilon_{-\sigma} + \Gamma_N/2}{(s-s_3)(s-s_4)\left(s + i\varepsilon_{k_2}\right)}\right\}(t)\left\langle c^+_{k_1\sigma}(0)c_{k_2\sigma}(0)\right\rangle \\
&+ \frac{\Gamma_{12}}{4}\sum_{k_1,k_2} V_{k_1}V_{k_2}\mathcal{L}^{-1}\left\{\frac{1}{(s-s_1)(s-s_2)\left(s + i\varepsilon_{k_1}\right)}\right\}(t)\mathcal{L}^{-1}\left\{\frac{1}{(s-s_3)(s-s_4)\left(s - i\varepsilon_{k_2}\right)}\right\}(t)\left\langle c_{k_1-\sigma}(0)c^+_{k_2-\sigma}(0)\right\rangle, \qquad (15)
\end{aligned}
$$

where $s_{1,2} = \frac{1}{2}[i(\varepsilon_\uparrow - \varepsilon_\downarrow) - \Gamma_N \pm i\sqrt{\delta}]$, and for $\sigma =\downarrow$ one should replace $(s_1, s_2) \leftrightarrow (s_3, s_4)$, respectively. The first two terms describe the transient QD charge oscillations which depend on the initial QD occupations. The last two terms (with the sums over k) are related to the normal lead and they give nonvanishing and nonoscillating contribution to $n_\sigma(t)$, regardless of the initial conditions. Note that in Eq. (15) the terms involving the expectation values of the product of electron annihilation and creation operators $c_{q_j\sigma}$ and $c^\dagger_{q_j\sigma}$ of the superconducting lead electrons do not appear. Such terms take, e.g., the following integral form (cf. Ref. [80]):

$$
\frac{\Gamma_S}{2\pi}\int_{-\infty}^{+\infty} d\varepsilon f_S(\varepsilon)\mathcal{L}^{-1}\left\{\frac{\left(s + i\varepsilon_\downarrow + \frac{\Gamma_N}{2}\right)(s + i\varepsilon)}{(s-s_1)(s-s_2)(s^2 + \varepsilon^2 + |\Delta_j|^2)}\right\}(t)\mathcal{L}^{-1}\left\{\frac{\left(s - i\varepsilon_\downarrow + \frac{\Gamma_N}{2}\right)(s - i\varepsilon)}{(s-s_3)(s-s_4)(s^2 + \varepsilon^2 + |\Delta_j|^2)}\right\}(t), \qquad (16)
$$

where $f_s(\varepsilon)$ is the Fermi distribution function. It is easy to check numerically that the above integral over the energy is smaller and smaller with increasing $|\Delta_j|$. Thus in our calculations for $|\Delta_j| = \infty$ we can neglect all terms involving operators $\hat{c}_{\mathbf{q}\sigma}(0)$. The formula (15) can be further elaborated and after some algebra one rewrites the two first terms explicitly while the third and fourth terms can be expressed by integrals over the energy in the normal lead spectrum

$$
\begin{aligned}
n_\sigma(t) = {}& e^{-\Gamma_N t}\left[n_\sigma(0) + (1 - n_\sigma(0) - n_{-\sigma}(0))\sin^2\left(\frac{\sqrt{\delta}t}{2}\right)\frac{\Gamma_{12}}{\delta}\right] \\
&+ \frac{\Gamma_N}{2\pi}\int_{-\infty}^{+\infty} d\varepsilon f_N(\varepsilon)\mathcal{L}^{-1}\left\{\frac{s + i\varepsilon_{-\sigma} + \Gamma_N/2}{(s-s_1)(s-s_2)(s - i\varepsilon)}\right\}(t)\cdot\mathcal{L}^{-1}\left\{\frac{s - i\varepsilon_{-\sigma} + \Gamma_N/2}{(s-s_3)(s-s_4)(s + i\varepsilon)}\right\}(t) \\
&+ \frac{\Gamma_N}{8\pi}\Gamma_{12}\int_{-\infty}^{+\infty} d\varepsilon(1 - f_N(\varepsilon))\mathcal{L}^{-1}\left\{\frac{1}{(s-s_1)(s-s_2)(s + i\varepsilon)}\right\}(t)\cdot\mathcal{L}^{-1}\left\{\frac{1}{(s-s_3)(s-s_4)(s - i\varepsilon)}\right\}(t). \qquad (17)
\end{aligned}
$$

Here $f_N(\varepsilon)$ is the electron Fermi distribution function for the normal lead and for $\sigma = \downarrow$ the replacement $(s_1, s_2) \leftrightarrow (s_3, s_4)$ should be done. The phase difference $\phi = \phi_1 - \phi_2$ enters Eq. (17) only through the function $\cos\phi$, therefore the QD occupancy satisfies the symmetry relation $n_\sigma(\phi) = n_\sigma(\phi + 2\pi)$. Note that the part which depends on the initial QD filling oscillates with the period $2\pi/\sqrt{\delta}$. These oscillations depend on the QD electron energies, $\varepsilon_\uparrow + \varepsilon_\downarrow$, both couplings Γ_{S_1}, Γ_{S_2}, and the phase difference ϕ of the superconducting order parameters, $\phi = \varphi_1 - \varphi_2$. The oscillations are damped due to the exponential factor $e^{-\Gamma_N t}$ and in the asymptotic time limit the information about the initial QD occupation is entirely washed out. From Eq. (17) we infer that, when QD is coupled only to the superconducting leads and the initial conditions are $n_\sigma(0) = (1, 0)$ or (0,1), the time-dependent QD occupancy does not change at all (independently of ϕ and $\Gamma_{S_{1/2}}$). In this case the QD is occupied only be one electron which cannot be exchanged with the superconducting reservoirs due to the infinity large energy gaps. For the initial conditions $n_\sigma(0) = (1, 1)$ or $(0, 0)$ the QD occupancy oscillates with the time period $T = \frac{2\pi}{\sqrt{\delta}}$ for $\phi \neq \pi$ independently of $\Gamma_{S_{1/2}}$ or for $\phi = \pi$, $\Gamma_{S_1} \neq \Gamma_{S_2}$. These oscillations, however, disappear for $\phi = \pi$ and $\Gamma_{S_1} = \Gamma_{S_2}$ as shown in Fig. 2.

The formula (17) for $\Gamma_N = 0$ resembles the Rabbi oscillations of a typical two-level quantum system described by the effective Hamiltonian $H_{\text{eff}} = \frac{1}{2}(\Gamma_{S_1}e^{i\varphi_1} + \Gamma_{S_2}e^{i\varphi_2})c^\dagger_\uparrow c^\dagger_\downarrow +$ H.c. $+ \sum_\sigma \varepsilon_\sigma n_\sigma$. Assuming that at $t = 0$ the QD is empty, $n_\sigma(0) = 0$, we can calculate the probability $P(t)$ of finding

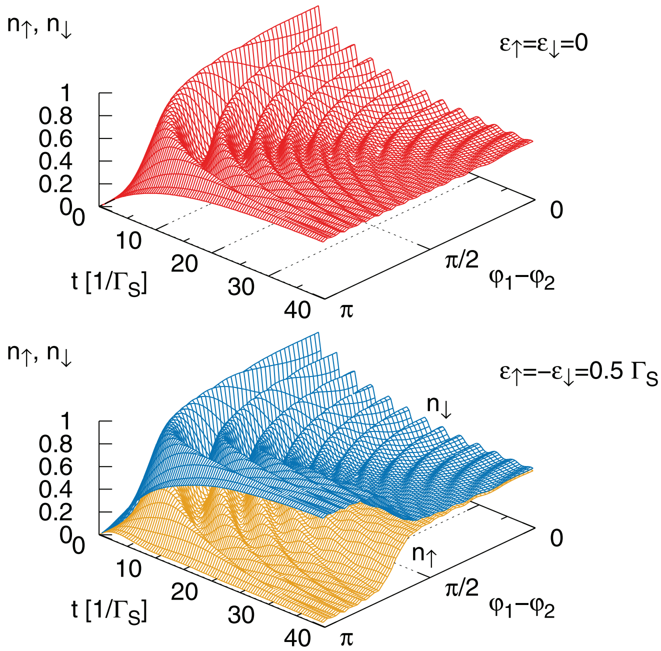

FIG. 2. Time evolution of the QD occupancies $n_\uparrow(t)$, $n_\downarrow(t)$ as a function of the phase difference ϕ for $\varepsilon_\sigma = 0$ (upper panel) and $\varepsilon_\uparrow = -\varepsilon_\downarrow = 0.5$ (bottom panel). $\Gamma_{S1} = \Gamma_{S2} = \Gamma_S = 1$, $\Gamma_N = 0.1$, $\mu_N = 0$, $|\Delta_1| = |\Delta_2| \to \infty$, $n_\sigma(0) = 0$. The QD occupancies satisfy the relation $n_\sigma(\phi) = n_\sigma(\phi + 2\pi)$ and for $t = \infty$ are symmetrical with regard to $\phi = \pi$.

the QD in the doubly occupied configuration, $n_\uparrow = n_\downarrow = 1$. Within the standard treatment of a two-level system we have [80,99]

$$P(t) = \frac{\Gamma_{12}}{\Gamma_{12} + (E_1 - E_2)^2} \sin^2\left(\sqrt{\Gamma_{12} + (E_1 - E_2)^2}\,\frac{t}{2}\right), \tag{18}$$

where $E_1 = 0$ and $E_2 = \varepsilon_\uparrow + \varepsilon_\downarrow$ are energies of the empty and double occupied configurations, respectively. This formula can be rewritten as $P(t) = \frac{\Gamma_{12}}{\delta} \sin^2(\frac{\sqrt{\delta}}{2} t)$ and becomes identical with our expression (17) obtained for $n_\sigma(0) = 0$, $\Gamma_N = 0$.

To illustrate such analytical results and to reveal influence of the phase difference of two superconducting leads on the QD occupation in Fig. 2 we show $n_\uparrow(t)$ and $n_\downarrow(t)$ with respect to time and ϕ for $\varepsilon_\sigma = 0$ (upper panel) and for the Zeeman splitting $\varepsilon_\sigma = -\varepsilon_{-\sigma} = 0.5$ (bottom panel). We consider here the symmetric coupling $\Gamma_{S_1} = \Gamma_{S_1} = \Gamma_S$ and assume the initial conditions $n_\sigma(0) = (0, 0)$. Note that for $\varepsilon_\sigma = 0$ the QD occupancy becomes spin independent, i.e., $n_\sigma(t) = n_{-\sigma}(t)$ [see Eq. (17)]. For $t \to \infty$ it always tends to 0.5, regardless of the superconducting phase difference. In the absence of any phase difference we observe the oscillations of $n_\sigma(t)$ with the period $T = \pi/\Gamma_S$ which are damped according to the exponential function $e^{-\Gamma_N t}$. Notice that the period of these oscillations is twice as short compared to the oscillations in the N-QD-S system [80]. For $\phi \neq 0$ these oscillations are characterized by the phase-dependent period $T = \pi/[\Gamma_S|\cos(\phi/2)|]$. For the special case $\phi = \pi$ ($\Gamma_{12} = 0$) the oscillations disappear and the QD charge develops in time exactly in the same way as for the QD coupled only to the normal lead (with $\varepsilon_\sigma = 0$), e.g., Ref. [1]:

$$n_\sigma(t) = n_\sigma(0)e^{-\Gamma_N t} + \frac{\Gamma_N}{\pi} e^{-\Gamma_N t/2} \times \int_{-\infty}^{+\infty} d\varepsilon f_N(\varepsilon) \frac{\cosh(\Gamma_N t/2) - \cos(\varepsilon t)}{(\Gamma_N/2)^2 + \varepsilon^2}. \tag{19}$$

For $\mu = 0$ and the zero temperature case we obtain $n_\sigma(t) = \frac{1}{2} + e^{-\Gamma_N t}(n_\sigma(0) - \frac{1}{2})$. It means that for $n_\sigma(0) = (0, 0)$ or (1,1) the QD occupation increases or decreases monotonically in time without any oscillations, changing from zero (one) to 0.5 (see Fig. 2, upper panel).

The situation changes in the presence of the Zeeman splitting (bottom panel). For symmetric splitting around $\mu_N = 0$, $\varepsilon_\uparrow = -\varepsilon_\downarrow$, the first term of Eq. (17) depends only on the phase difference ϕ and Γ_{S_i}. Its contribution to the final QD occupancy is the same for arbitrary values of ε_σ. On the other hand the two last terms in Eq. (17) depend separately on ε_σ. For $\phi = \pi$ the contribution from these terms is identical with the case of the QD coupled only to the normal lead. For $t = 40$ and $\varepsilon_\uparrow = -\varepsilon_\downarrow = 0.5$ (bottom panel in Fig. 2), the contribution for spin up (down) is $\sim$0.03 ($\sim$0.95). For $\phi = 0$ such contributions become $\sim$0.49 and $\sim$0.51, respectively. One can thus control the QD occupancy by changing the phase difference ϕ.

Let us analyze more carefully variation of the QD occupancy against the phase difference ϕ. In Fig. 3 (upper panel) we present the ABS energies of the proximitized QD, $E_{\alpha\beta} = \bar{E}_\alpha - \varepsilon_\beta$, ($\alpha = \pm$, $\beta = \pm \equiv \uparrow/\downarrow$), where $\bar{E}_\alpha = \frac{1}{2}(\varepsilon_\uparrow + \varepsilon_\downarrow) + \alpha\sqrt{\frac{(\varepsilon_\uparrow + \varepsilon_\downarrow)^2}{4} + \Gamma_S^2 \cos^2\frac{\phi}{2}}$ is the quasiparticle energy, representing a superposition of the empty and double occupied states [100]. In the lower panel we show the QD occupancies $n_\uparrow(t)$, $n_\downarrow(t)$ and the difference $n_\downarrow(t) - n_\uparrow(t)$ for $\Gamma_N = 0.02$ obtained for particular times t. QD occupancy rapidly changes for such values of ϕ which satisfy the relation $E_{++} = E_{--}$, i.e., for $\phi = \pi \pm \arccos\frac{\varepsilon_\uparrow}{\Gamma_S}$ (here $\varepsilon_\uparrow + \varepsilon_\downarrow = 0$, $\varepsilon_\uparrow > 0$). Exactly for such values of ϕ we observe an abrupt change of the QD magnetization, which is well visible especially in the long-time (steady) limit. In our case for $\Gamma_N = 0.02$ this time equals 200 u.t. (approximately equal to $\frac{4}{\Gamma_N}$). For stronger couplings Γ_N such changeover of the QD magnetization is also observed (not shown here) although it is more smeared around $\phi = \pi \pm \pi/3$ even for longer time after the quench. At a very early stage of the time evolution such a transition of the magnetization from zero value to 1 is only weakly manifested (see the upper thick red curve in the lower panel of Fig. 3). On the other hand, oscillations of the QD occupancies hardly detect the existence of this transition. However, already for $t \simeq \frac{1}{\Gamma_N} = 50$ u.t. this transition is well marked on the occupancy curves as well as on $n_\downarrow(t) - n_\uparrow(t)$. Notice the decreasing amplitude and increasing frequency of the QD occupancies versus time. These transient characteristics are described by the factor $\sin^2(2\Gamma_S|\cos(\phi/2)|t)e^{-\Gamma_N t}$, see the first term of Eq. 17. Let us emphasize, that despite oscillatory character of $n_\sigma(t)$, the resulting magnetization $n_\downarrow(t) - n_\uparrow(t)$ is a smooth function of ϕ.

IV. INDUCED ON-DOT PAIRING

We shall now calculate the pairing amplitude $\chi(t) \equiv \langle c_\downarrow(t) c_\uparrow(t)\rangle$ driven by the proximity effect, assuming absence

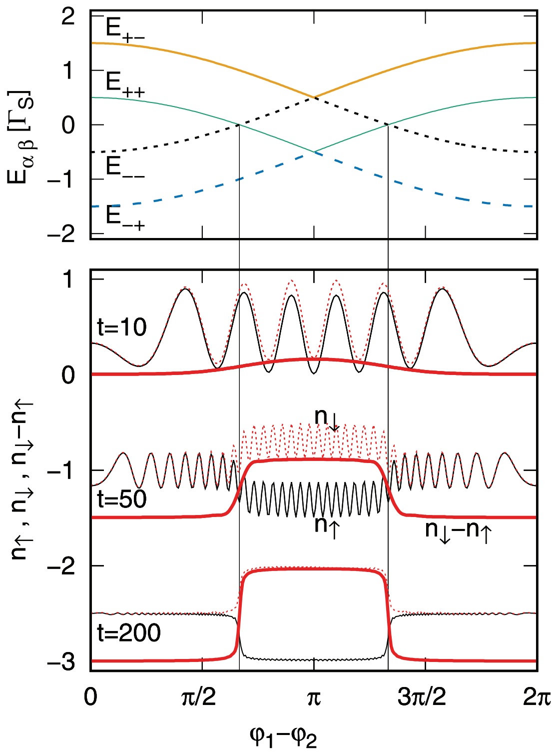

FIG. 3. Energies of the subgap quasiparticles of the proximitized QD, $E_{\alpha\beta}$, (upper panel) and QD occupancies: $n_\uparrow$, $n_\downarrow$, and $n_\downarrow - n_\uparrow$ (solid black, broken red, and thick red curves, respectively) as a function of ϕ. The occupancies are obtained for $t = 10$, $t = 50$ (shifted down by 1.5) and for $t = 200$ u.t. (shifted down by 3.0). The vertical black lines indicate characteristic points for $\phi = \frac{2\pi}{3}$ and $\phi = \frac{4\pi}{3}$, and the other parameters are $\varepsilon_\uparrow = -\varepsilon_\downarrow = 0.5$, $\Gamma_{S1} = \Gamma_{S2} = \Gamma_S = 1$, $\Gamma_N = 0.02$, $\mu_N = 0$.

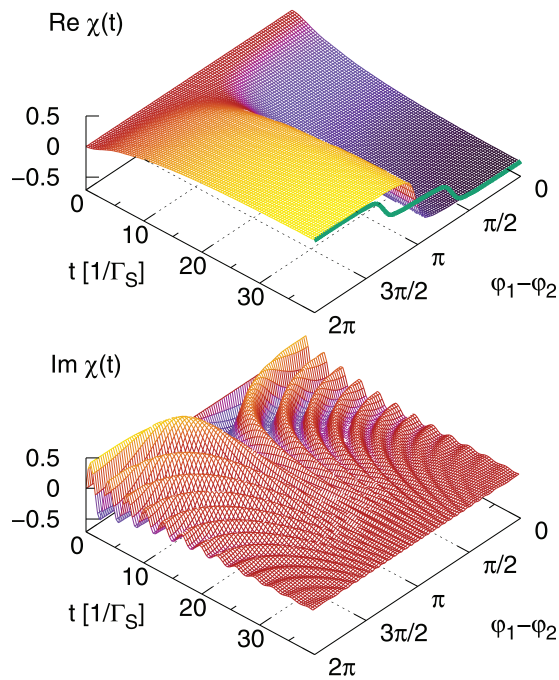

FIG. 4. The real (upper panel) and imaginary (bottom panel) parts of the QD induced pairing $\chi(t) = \langle c_\downarrow(t)c_\uparrow(t)\rangle$ as a function of time and the phase difference $\varphi_1 - \varphi_2$ for $\varepsilon_\sigma = 0$, $\Gamma_{S_1} = \Gamma_{S_2} = \Gamma_S$, $\Gamma_N = 0.1$, and $n_\sigma(0) = 0$. $\chi(t)$ satisfies the relation $\chi(t,\phi) = \chi(t,\phi + 4\pi)$ and for $t = \infty$ is symmetrical about $\phi = 2\pi$. The bold green line for $t = 40$ in the upper panel corresponds to the case $\varepsilon_\uparrow = -\varepsilon_\downarrow = 0.5$.

of any bias voltage ($\mu_N = 0$). Using the expressions for $c_\uparrow(s)$ and $c_\downarrow(s)$ obtained in Sec. II we find

$$\begin{aligned}\chi(t) = &-\frac{i}{2}(\Gamma_{S1}e^{i\varphi_1} + \Gamma_{S2}e^{i\varphi_2})\left[-n_\uparrow(0)\mathcal{L}^{-1}\left\{\frac{1}{(s-s_1)(s-s_2)}\right\}(t)\right.\\ &\times\mathcal{L}^{-1}\left\{\frac{s - i\varepsilon_\downarrow + \Gamma_N/2}{(s-s_3)(s-s_4)}\right\}(t)\\ &+(1-n_\downarrow(0))\mathcal{L}^{-1}\left\{\frac{s - i\varepsilon_\uparrow + \Gamma_N/2}{(s-s_1)(s-s_2)}\right\}(t)\\ &\left.\times\mathcal{L}^{-1}\left\{\frac{1}{(s-s_3)(s-s_4)}\right\}(t) + \frac{\Gamma_N}{2\pi}\Phi_\uparrow^*\right]\end{aligned} \tag{20}$$

where

$$\begin{aligned}\Phi_\sigma = &\int_{-\infty}^{+\infty} d\varepsilon\mathcal{L}^{-1}\left\{\frac{1}{(s-s_1)(s-s_2)(s+i\varepsilon)}\right\}(t)\\ &\times\mathcal{L}^{-1}\left\{\frac{s + i\varepsilon_\sigma + \Gamma_N/2}{(s-s_3)(s-s_4)(s-i\varepsilon)}\right\}(t)(1-f_N(\varepsilon))\\ &-\int_{-\infty}^{+\infty} d\varepsilon f_N(\varepsilon)\mathcal{L}^{-1}\left\{\frac{s + i\varepsilon_{-\sigma} + \Gamma_N/2}{(s-s_1)(s-s_2)(s-i\varepsilon)}\right\}(t)\\ &\times\mathcal{L}^{-1}\left\{\frac{1}{(s-s_3)(s-s_4)(s+i\varepsilon)}\right\}(t),\end{aligned} \tag{21}$$

and the replacement $(s_1, s_2) \to (s_3, s_4)$ should be made for $\sigma = \downarrow$. The terms proportional to $n_\uparrow(0)$ and $(1 - n_\downarrow(0))$ in the above relation can be expressed analytically, and

$$\begin{aligned}\chi(t) = &\frac{i}{2}(\Gamma_{S_1}e^{i\varphi_1} + \Gamma_{S_2}e^{i\varphi_2})\\ &\times\left\{-\frac{\Gamma_N}{2\pi}\Phi_\uparrow^* + (n_\downarrow(0) + n_\uparrow(0) - 1)e^{-\Gamma_N t}\right.\\ &\left.\times[\sqrt{\delta}\sin(\sqrt{\delta}t) + i(\varepsilon_\uparrow + \varepsilon_\downarrow)(\cos(\sqrt{\delta}t) - 1)]\Big/\delta\right\}.\end{aligned} \tag{22}$$

Notice, that for $\Gamma_{S_1} = \Gamma_{S_2} = \Gamma_S$ and $\phi = \pi$ the factor $\Gamma_{S_1}e^{i\varphi_1} + \Gamma_{S_2}e^{i\varphi_2} = 2\Gamma_S\cos\frac{\phi}{2}$ vanishes, therefore the on-dot pairing $\langle c_\downarrow(t)c_\uparrow(t)\rangle$ is absent (see upper and bottom panels in Fig. 4 for $\phi = \pi$). However, for $\phi \neq \pi$ and $\varepsilon_\uparrow + \varepsilon_\downarrow = 0$ we have

$$\begin{aligned}\chi(t) = &-\frac{\Gamma_N\Gamma_S}{2\pi}\cos\frac{\phi}{2}\Im\Phi_\uparrow + \frac{i}{2}(n_\downarrow(0) + n_\uparrow(0) - 1)\\ &\times e^{-\Gamma_N t}\frac{\cos\frac{\phi}{2}}{|\cos\frac{\phi}{2}|}\sin\left(2\Gamma_S|\cos\frac{\phi}{2}|t\right),\end{aligned} \tag{23}$$

where we have used the property $\Re\Phi_\sigma = 0$, corresponding to $\mu_N = 0$ [80]. The imaginary part of $\chi(t)$ oscillates with the same period as the QD occupancy, i.e., with $T = \pi/[\Gamma_S|\cos(\phi/2)|]$, but the real part changes monotonically from zero to some constant value without any oscillations (upper panel). We can notice that the imaginary part of χ

vanishes when the QD is filled by a single electron at the initial time $t = 0$. On the other hand, the real part of χ is a nonvanishing function irrespective of the initial conditions. It is worth mentioning that for $\Gamma_N = 0$ (i.e., Josephson junction setup) and for $\varepsilon_\uparrow + \varepsilon_\downarrow = 0$ the expression for $\chi(t)$ becomes purely imaginary and is characterized by undamped oscillations inducing d.c. current (see Sec. V). In general, from the analysis of Eq. (20) we infer that the QD induced pairing satisfies the symmetry relation $\chi(t,\phi) = \chi(t,\phi+4\pi)$. In particular, for $t=\infty$, it becomes symmetric with respect to $\phi = 2\pi$.

V. SUBGAP CURRENTS

Let us consider the currents $j_{N\sigma}(t)$ and $j_{Sj\sigma}(t)$ flowing between the QD and the normal or superconducting electrodes, respectively. These currents depend on time due to the abrupt coupling of all parts of the considered system. For $t > 0$, even at zero bias voltage, there are induced transient currents. Such electron currents can be obtained from the evolution of the total number of electrons of the corresponding electrode [1]. For the normal lead we can express it as [38,50,51,57,68]:

$$j_{N\sigma}(t) = 2\Im\left(\sum_k V_{k\sigma} e^{-i\varepsilon_{k\sigma}t} \langle c_\sigma^+(t) c_{k\sigma}(0)\rangle\right) - \Gamma_N n_\sigma(t), \quad (24)$$

where we have assumed the energy-independent normal lead spectrum. Using the formulas of Sec. II we find

$$j_{N\sigma}(t) = \frac{\Gamma_N}{\pi}\Re\left(\int_{-\infty}^{+\infty} d\varepsilon f_N(\varepsilon) e^{-i\varepsilon t} \times \mathcal{L}^{-1}\left\{\frac{s+i\varepsilon_{-\sigma}+\Gamma_N/2}{(s-s_1)(s-s_2)(s-i\varepsilon)}\right\}(t)\right) - \Gamma_N n_\sigma(t). \quad (25)$$

Inserting the inverse Laplace transform and using the expression for $n_\sigma(t)$ one can obtain the analytical relation for $j_{N\sigma}(t)$. However, this solution for arbitrary t cannot be written in relatively compact (or transparent) form, so we restrict ourselves to the asymptotics $t = \infty$

$$\begin{aligned} j_{N\sigma} = \frac{\Gamma_N}{\pi}\int d\varepsilon \Bigg\{ f_N(\varepsilon)\Bigg[\Re\left(\frac{i(\varepsilon+\varepsilon_{-\sigma})+\frac{\Gamma_N}{2}}{\left(\frac{\Gamma_N}{2}+i\varepsilon_{++}\right)\left(\frac{\Gamma_N}{2}+i\varepsilon_{-+}\right)}\right) \\ - \frac{\Gamma_N}{2}\frac{(\varepsilon+\varepsilon_{-\sigma})^2+\frac{\Gamma_N^2}{4}}{\left(\frac{\Gamma_N^2}{4}+\varepsilon_{++}^2\right)\left(\frac{\Gamma_N^2}{4}+\varepsilon_{-+}^2\right)}\Bigg] \\ - (1-f_N(\varepsilon))\frac{\Gamma_N\Gamma_{12}}{8\left(\frac{\Gamma_N^2}{4}+\varepsilon_{+-}^2\right)\left(\frac{\Gamma_N^2}{4}+\varepsilon_{--}^2\right)}\Bigg\}, \end{aligned} \quad (26)$$

where $\varepsilon_{\alpha\beta} = \varepsilon + E_{\alpha\beta}$ and $E_{\alpha\beta}$ are the quasiparticle energies of the proximitized QD.

Upper panel of Fig. 5 shows the time-dependent current flowing from the normal lead to the QD as a function of the phase difference $\phi = \varphi_1 - \varphi_2$ obtained for the unbiased system and $\varepsilon_\sigma = 0$. At the beginning the current starts to flow from the normal electrode to the empty QD. In a next stage, electrons tunnel in both directions with the characteristic oscillations. These damped oscillations are clearly visible and for $t \to \infty$ the current vanishes for all ϕ. The period of these oscillations increases with ϕ, similarly to the behavior observed for the QD occupancy. Exceptionally, for $\phi = \pi$, the current tends to its asymptotic value without any oscillations according to the formula (valid for the zero temperature, $\varepsilon_\sigma = 0$ and $\Gamma_{S_1} = \Gamma_{S_2}$):

$$j_{N\sigma}(t) = \Gamma_N e^{-\Gamma_N t}\left(\tfrac{1}{2} - n_\sigma(0)\right). \quad (27)$$

We can notice that right after the abrupt coupling (at $t = 0^+$) the large value of transient current $j_{N\sigma}$ is induced in the system ($\sim\frac{\Gamma_N}{2}$) which is artifact of the WBL approximation [15]. We have checked that by applying a more realistic (smooth) QD-leads coupling profile the initial current would gradually increase, revealing the same period of oscillations and other overall features [80].

The situation looks a bit different for the currents flowing between the QD and superconducting leads. To calculate these currents we start from the standard formula $j_{Sj\sigma}(t) = 2\Im(\sum_{qj} V_{qj}\langle c_\sigma^+(t) c_{qj\sigma}(t)\rangle)$ and use the Laplace transforms for $c_\sigma^+(s)$ and $c_{qj\sigma}(s)$, obtaining [80]

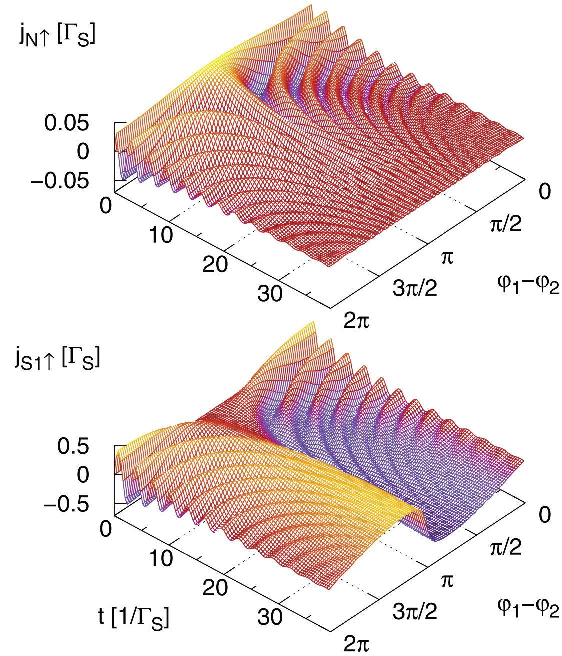

FIG. 5. The time dependent currents flowing between the QD and the normal lead, $j_{N\uparrow}(t)$ (upper panel), and between the QD and the superconducting lead, $j_{S1\uparrow}(t)$ (bottom panel), as a function of the phase difference $\varphi_1 - \varphi_2$. The system parameters are: $\varepsilon_\sigma = 0$, $\Gamma_{S_1} = \Gamma_{S_2} = \Gamma_S$, $\Gamma_N = 0.1$, and $n_\sigma(0) = 0$.

$$\begin{aligned} j_{S_{1/2}\sigma}(t) = \Re\Bigg\{\frac{\Gamma_{S_{1/2}}}{2}\left(\Gamma_{S_{1/2}} + \Gamma_{S_{2/1}} e^{\pm i\phi}\right)\Bigg[\frac{\Gamma_N}{2\pi}\Phi_\sigma - n_\sigma(0)\mathcal{L}^{-1}\left\{\frac{1}{(s-s_3)(s-s_4)}\right\}(t)\mathcal{L}^{-1}\left\{\frac{s+i\varepsilon_{-\sigma}+\Gamma_N/2}{(s-s_1)(s-s_2)}\right\}(t) \\ + (1-n_{-\sigma}(0))\mathcal{L}^{-1}\left\{\frac{1}{(s-s_1)(s-s_2)}\right\}(t)\mathcal{L}^{-1}\left\{\frac{s+i\varepsilon_\sigma+\Gamma_N/2}{(s-s_3)(s-s_4)}\right\}(t)\Bigg]\Bigg\}. \end{aligned} \quad (28)$$

As usually, the replacement $(s_1, s_2) \leftrightarrow (s_3, s_4)$ should be made for $\sigma = \downarrow$. After straightforward algebra we can derive more explicit form for the superconducting current

$$j_{S_{1/2}\sigma}(t) = \frac{\Gamma_{S_{1/2}}}{2\delta}(1 - n_\sigma(0) - n_{-\sigma}(0))e^{-\Gamma_N t}\big[\big(\Gamma_{S_{2/1}}\cos\phi + \Gamma_{S_{1/2}}\big)\sqrt{\delta}\sin(\sqrt{\delta}t) \mp \Gamma_{S_{2/1}}(\varepsilon_\sigma + \varepsilon_{-\sigma})\sin\phi(1 - \cos(\sqrt{\delta}t))\big] + \frac{\Gamma_N\Gamma_{S_{1/2}}}{4\pi}\Re\big\{\big(\Gamma_{S_{1/2}} + \Gamma_{S_{2/1}}e^{\pm i\phi}\big)\Phi_\sigma\big\}. \tag{29}$$

Using the relation for the induced pairing, Eq. (20), the above current can be recast as $j_{S_j\sigma}(t) = \Im(\Gamma_{S_j}e^{i\varphi_j}\langle c_\downarrow(t)c_\uparrow(t)\rangle^*)$. Assuming that $\langle c_\downarrow(t)c_\uparrow(t)\rangle = |\langle c_\downarrow(t)c_\uparrow(t)\rangle|e^{i\varphi_d}$, where φ_d is the argument (phase) of $\langle c_\downarrow(t)c_\uparrow(t)\rangle$, we obtain (e.g., Ref. [69]):

$$j_{S_j\sigma}(t) = \Gamma_{S_j}\,|\langle c_\downarrow(t)c_\uparrow(t)\rangle|\,\sin(\varphi_j - \varphi_d), \tag{30}$$

where $j = 1, 2$. Inspecting (30) we conclude that the currents flowing between the QD and a given superconducting lead does not depend on spin, $j_{S_{1\sigma}}(t) = j_{S_{1-\sigma}}(t)$, irrespective of the spin dependent QD energy levels. This is a consequence of the fact that the QD can exchange charge with the superconducting leads only via pairs of opposite spin electrons.

Formula (30) simplifies for the case $\Gamma_{S_1} = \Gamma_{S_2} \equiv \Gamma_S$ and $\varepsilon_\uparrow + \varepsilon_\downarrow = 0$, when we obtain

$$\begin{aligned} j_{S_1\sigma}(t) = {} & \frac{\Gamma_S}{2}e^{-\Gamma_N t}[1 - n_\sigma(0) - n_{-\sigma}(0)] \\ & \times\cos(\phi/2)\,\sin(2\Gamma_S|\cos(\phi/2)|t) \\ & + \frac{\Gamma_N\Gamma_S^2}{2\pi}\cos^2(\phi/2)\Re\{\Phi_\sigma\} - \frac{\Gamma_N\Gamma_S^2}{4\pi}\sin\phi\,\Im\{\Phi_\sigma\}. \end{aligned} \tag{31}$$

For $\mu_N = 0$ the real part of Φ_σ, $\Re\{\Phi_\sigma\}$, vanishes [80] and in such a case for $\phi = \pi$ and identical couplings to both superconducting leads the currents $j_{S_j\sigma}(t)$ vanish.

Under nonequilibrium conditions ($\mu_N \neq 0$) for symmetric couplings and assuming $\varepsilon_\uparrow = -\varepsilon_\downarrow$, the asymptotic ($t \to \infty$) value of the superconducting current can be expressed as

$$\begin{aligned} j_{S_1\sigma} = {} & \frac{\Gamma_N^2\Gamma_S^2}{4\pi}\left\{\int\frac{(1 - f_N(\varepsilon))d\varepsilon}{[(\Gamma_N^2/4 + \varepsilon_{+-}^2)][(\Gamma_N^2/4 + \varepsilon_{--}^2)]}\right. \\ & \left. - \int\frac{f_N(\varepsilon)d\varepsilon}{[(\Gamma_N^2/4 + \varepsilon_{-+}^2)][(\Gamma_N^2/4 + \varepsilon_{++}^2)]}\right\}\cos^2\left(\frac{\phi}{2}\right) \\ & - \frac{\Gamma_N\Gamma_S^2}{4\pi}\left\{\int\frac{(1 - f_N(\varepsilon))(\varepsilon + \varepsilon_\uparrow)d\varepsilon}{[(\Gamma_N^2/4 + \varepsilon_{+-}^2)][(\Gamma_N^2/4 + \varepsilon_{--}^2)]}\right. \\ & \left. - \int\frac{f_N(\varepsilon)(\varepsilon - \varepsilon_\uparrow)d\varepsilon}{[(\Gamma_N^2/4 + \varepsilon_{-+}^2)][(\Gamma_N^2/4 + \varepsilon_{++}^2)]}\right\}\sin\phi \end{aligned} \tag{32}$$

where $\varepsilon_{\alpha\beta} = \varepsilon + E_{\alpha\beta}$ and $E_{\alpha\beta}$ denote quasiparticle energies of the proximitized QD. Notice that the first term in the above formula vanishes for zero temperature and $\mu_N = 0$. In this case the superconducting current can be rewritten to the following (Josephson-like) formula

$$j_{S_1\sigma} = \frac{\Gamma_S}{4\pi}\frac{\sin\phi}{|\cos\left(\frac{\phi}{2}\right)|}\left[\arctan\frac{\varepsilon_\uparrow^2 + \frac{\Gamma_N^2}{4} - \Gamma_S^2\cos^2\left(\frac{\phi}{2}\right)}{\Gamma_S\Gamma_N|\cos\left(\frac{\phi}{2}\right)|} - \frac{\pi}{2}\right]. \tag{33}$$

Let us remark that the formula for the current, Eq. (31), can be used to determine the coupling value Γ_S. As the time oscillations are described by the first term of Eq. (31), then for a given ϕ the oscillating part of $j_{S_j\sigma}(t)$ is proportional to $\sin(2\Gamma_S|\cos(\phi/2)|t)$. The period of these oscillations $T = \frac{\pi}{\Gamma_S|\cos(\phi/2)|}$ for the system characterized by a sufficiently small Γ_S and $\phi \simeq \pi$ should be experimentally detectable.

Lower panel in Fig. 5 presents the current $j_{S_1\uparrow}(t)$ as a function of ϕ for $n_\uparrow(0) = n_\downarrow(0) = 0$. The current oscillates with a damping amplitude and for large time it tends to a nonzero asymptotic value given in Eq. (33). The asymptotic value of the current does not depend on the initial QD occupancies, see Eq. (29). However, the transient currents are different for the QD initial occupancies, $n_\sigma(0) = (0, 0)$, (1,1) and for $n_\sigma(0) = (0, 1)$, (1,0). In the first case the current indicates a rather rich time-dependent structure before it attains the asymptotic value. This is a consequence of the Rabi-like oscillations (damped via $e^{-\Gamma_N t}$ due to the coupling with normal lead) between the empty and double occupied QD configurations and is described by the first term of Eq. (29) which depends on the factor $(1 - n_\sigma(0) - n_{-\sigma}(0))$. This factor disappears for the initial occupancies $n_\sigma(0) = (0, 1)$ or (1,0) and all time dependence of $j_{S_i\sigma}(t)$ is described by the last term of Eq. (29). This term, however, in contrast to the former case does not introduce any visible oscillations for small Γ_N but enters the formulas for $j_{S_i\sigma}$, irrespective of the initial conditions. From Fig. 5 we can learn that at a short time after the quench the current is symmetric with respect to $\phi = \pi$. This symmetry, however, is quickly lost in the long time scale.

In Fig. 6 we present time dependent currents $j_{S_1\uparrow}$ and $j_{S_2\uparrow}$ vs the phase difference ϕ for the finite Zeeman splitting of energy levels, $\varepsilon_\uparrow = -\varepsilon_\downarrow = 0.5\Gamma_S$. Both currents oscillate with the period dependent on the phase difference ϕ. As before, this period increases with ϕ and for $\phi = \pi$ the currents do not flow in the system. Comparing such ϕ dependence of the currents with those presented in Fig. 5 (lower panel) for $\varepsilon_\sigma = 0$ we observe a different behavior, especially at asymptotic large time. In the presence of the Zeeman splitting the asymptotic currents almost vanish for some ϕ interval around $\phi = \pi$. To study this effect in more detail we show in Fig. 6, bottom panel, the superconducting currents for several values of the Zeeman splittings (solid lines for $\varepsilon_\uparrow = -\varepsilon_\downarrow = 0, 0.25, 0.5, 0.75$, and 1.0 expressed in units of Γ_S). As one can see, in the absence of the Zeeman splitting the current does not flow only for $\phi = 0, \pi$. In the presence of the Zeeman term the zero-value superconducting current interval of ϕ increases, but at the same time the maximal values of the currents diminish. For $\varepsilon_\uparrow = -\varepsilon_\downarrow \gg 1$ the superconducting currents do not flow. The corresponding asymptotic occupancies of the QD, $n_\uparrow(\phi, t = \infty)$, are shown in Fig. 6, bottom panel (broken lines). One can notice that

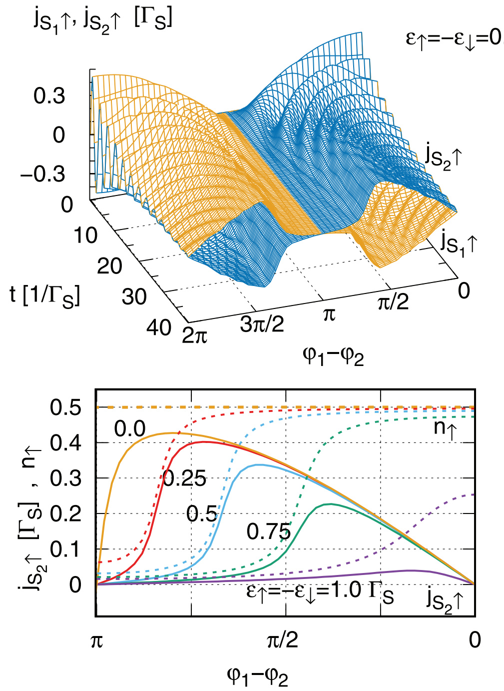

FIG. 6. Time dependent currents flowing between the QD and the superconducting leads, $j_{S_1\uparrow}(t)$, $j_{S_2\uparrow}(t)$ as a function of the phase difference $\varphi_1-\varphi_2$ in the presence of the Zeeman splitting $\varepsilon_\uparrow = -\varepsilon_\downarrow = 0.5$ (upper panel). In the bottom panel the asymptotic spin up currents (solid curves) and corresponding QD occupancies (broken curves) obtained for $t=\infty$ are shown for the Zeeman splitting: $\varepsilon_\uparrow = -\varepsilon_\downarrow = 0, 0.25, 0.5, 0.75$ and 1.0. The parameters are: $\Gamma_{S_1} = \Gamma_{S_2} = \Gamma_S$, $\Gamma_N = 0.2$, and $n_\sigma(0) = 0$.

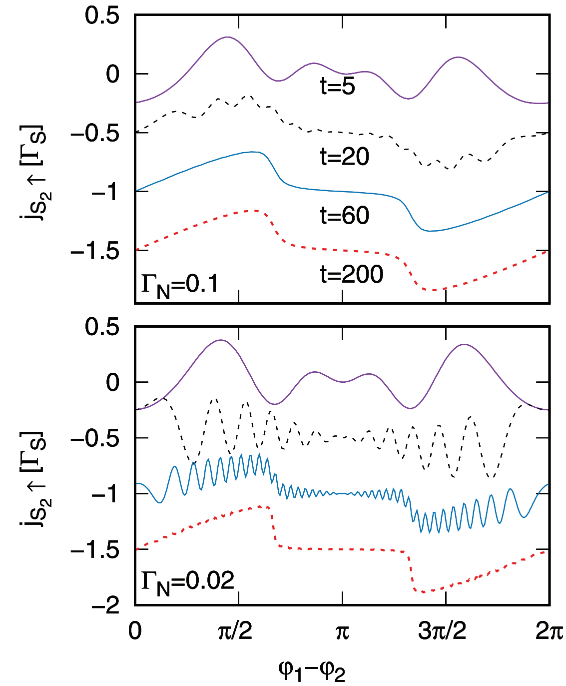

FIG. 7. The current $j_{S_2\uparrow}(t)$ as a function of the phase difference $\varphi_1-\varphi_2$ for different times: $t = 5, 20, 60$ and 200 u.t. (from upper to bottom curves in both panels, respectively). The upper (bottom) panel corresponds to $\Gamma_N = 0.1(0.02)$ and the Zeeman splitting is $\varepsilon_\uparrow = -\varepsilon_\downarrow = 0.5$, $\Gamma_{S_1} = \Gamma_{S_2} = \Gamma_S$, and $n_\sigma(0) = 0$. The curves for $t = 20, 60, 200$ are shifted down by 0.5, 1.0, 1.5, respectively, for better visualization.

the occupancies decrease monotonically with ϕ and remain very low for the zero-current interval of ϕ. The changes of the QD occupancies in the presence of the Zeeman splitting reflect phasal dependence of the superconducting currents. These changes are coordinated with the QD magnetization and will be discussed in the next paragraph (compare also ϕ dependence of $n_\uparrow$ for $\varepsilon_\uparrow = -\varepsilon_\downarrow = 0.5$ and $\Gamma_N = 0.1$ shown in the lower panel of Fig. 3).

In Fig. 7 we analyze the time dependence of $j_{S_2\sigma}(t)$ for some selected values of time t, starting from the quench at $t=0$ until nearly the asymptotically large times. In the lower panel, $\Gamma_N = 0.02$, the ϕ dependence of the current demonstrates abrupt changing of the current value at points corresponding to $E_{++} = E_{--}$ (see upper panel in Fig. 3). These jumps of the current are clearly visible for large times. However, for larger Γ_N, e.g., for $\Gamma_N = 0.1$ (upper panel, Fig. 7) the ϕ dependence of the current even for asymptotically large times does not show such sharp changes. Notice that the time at which the current achieves constant (in time) values is much shorter in comparison to the case of $\Gamma_N = 0.02$. In both regimes of Γ_N we can estimate this time as $\frac{4}{\Gamma_N}$ [compare the results for ϕ dependence of $n_\sigma(t)$]. For small time the abrupt change of the current is not visible but for larger time it becomes evident in spite of the oscillations. Such a transition is very well visible in the asymptotics, where the oscillations vanish. For larger Γ_N the current tends to its asymptotic value (without time oscillations) in much shorter time than for smaller Γ_N, due to the damping factor $e^{-\Gamma_N t}$ [see the first term in Eq. (31)].

Let us consider the simple case of the QD coupled solely to superconducting leads, assuming $\Gamma_{S_1} = \Gamma_{S_2} = \Gamma_S$, $\varepsilon_\uparrow = -\varepsilon_\downarrow$ and $n_\uparrow(0) = n_\downarrow(0) = 0$. In this case

$$n_\sigma(t) = \sin^2(\Gamma_S \cos(\phi/2)t), \tag{34}$$

$$j_{S_{1/2}\sigma}(t) = \frac{\Gamma_S}{2}\cos(\phi/2)\sin(2\Gamma_S|\cos(\phi/2)|t). \tag{35}$$

The QD occupancy and the current do not depend on spin and, in addition, both superconducting currents, $j_{S_{1/2}\sigma}(t)$, are exactly identical. Note, however, that for $\varepsilon_\uparrow + \varepsilon_\downarrow \neq 0$ these currents differ one from another, see Eq. (29), and their difference equals $\Gamma_S^2 \sin\phi\,(1-\cos(\sqrt{\delta}\,t))(\varepsilon_\uparrow+\varepsilon_\downarrow)/\delta$. The current $j_{S_j\sigma}$ vanishes for $\phi = \pi$ and $\Gamma_{S_1} = \Gamma_{S_2}$. For different couplings, $\Gamma_{S_1} \neq \Gamma_{S_2}$, the current does not vanish, even for $\phi = \pi$. For instance $j_{S_1\sigma}$ in this case (for $\varepsilon_\sigma = 0$) is found to be $j_{S_1\sigma}(t) = \frac{\Gamma_{S_1}}{2}\sin[(\Gamma_{S_1} - \Gamma_{S_2})t]$.

It would be interesting to consider the transition from the permanently oscillating superconducting currents in the system of the QD placed only between two superconducting leads ($\Gamma_N = 0$) to finite constant asymptotic values of such currents in the presence of the third normal lead ($\Gamma_N \neq 0$), see, e.g., the bottom panel in Fig. 6. From Eq. (31) we see that for $\Gamma_N \neq 0$ the current consists of two parts. The first one corresponds to the transient oscillations damped by the factor $e^{-\Gamma_N t}$, whereas the second one is described by the imaginary part of Φ_σ. This part of the current slowly evolves

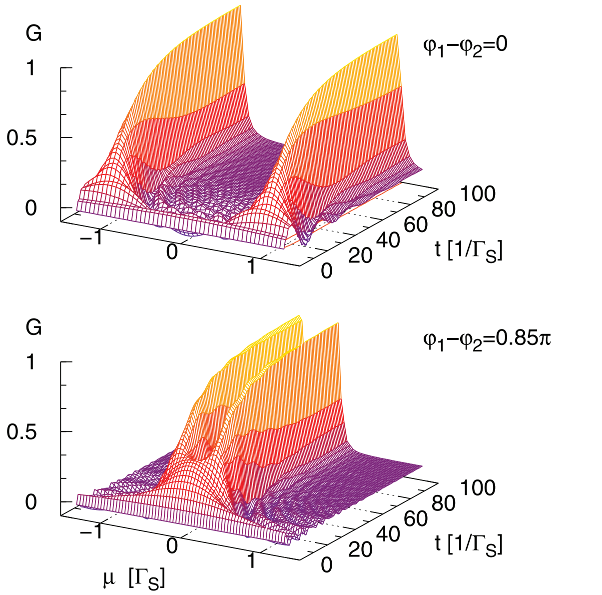

FIG. 8. Time-dependent Andreev conductance (in $4e^2/h$ units) as a function of the bias voltage μ for the phase difference $\phi = \varphi_1 - \varphi_2 = 0$ (upper panel) and for $\phi = 0.85\pi$ (bottom panel). The other system parameters are the same as in Fig. 2 with $\varepsilon_\sigma = 0$.

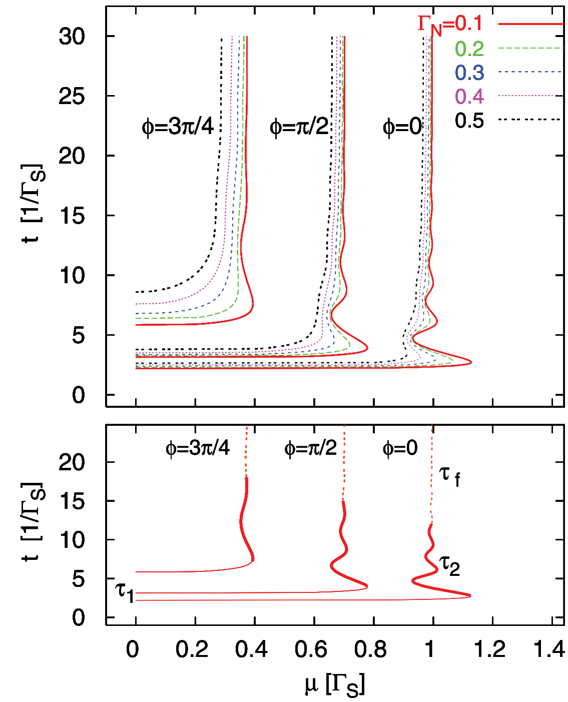

FIG. 9. Positions of the quasiparticle maxima vs time and μ appearing in the differential conductance $G_\sigma(\mu, t)$ for different Γ_N indicated in the legend and for superconducting phase difference $\phi = 0, \pi/2$ and $3\pi/4$, respectively (upper panel). The bottom panel shows the result for $\Gamma_N = 0.1$ where different time scales, τ_1, τ_2, and τ_f are indicated. For negative values of μ the results are symmetrical. The QD energy levels are: $\varepsilon_\sigma = 0$ and $\Gamma_{S_1} = \Gamma_{S_2} = \Gamma_S$.

in time to some nonzero asymptotic value given in Eq. (33). Asymptotic value of this current vanishes with decreasing Γ_N, but the oscillating part of the current is damped less and less effectively, and simultaneously the imaginary part of Φ_σ vanishes thereby the current oscillates with constant amplitude $\frac{\Gamma_S}{2}\cos(\phi/2)$, Eq. (31).

VI. DIFFERENTIAL SUBGAP CONDUCTANCE

The next part of our studies is devoted to the subgap time-dependent Andreev conductance $G_\sigma(\mu, t) = \frac{\partial}{\partial\mu} j_{N\sigma}(t)$, expressing it in units of $\frac{4e^2}{h}$. We investigate this quantity as a function of the bias voltage ($\mu = \mu_N$) applied to the normal lead. Using the expressions for the current and QD charge, Eqs. (17) and (25), we obtain at zero temperature

$$\begin{aligned} G_\sigma(\mu, t) = \Re\Bigg[\Gamma_N e^{-i\mu t}\mathcal{L}^{-1}\left\{\frac{s + i\varepsilon_{-\sigma} + \Gamma_N/2}{(s - s_1)(s - s_2)(s - i\mu)}\right\}(t)\Bigg] \\ + \frac{\Gamma_N^2\Gamma_{12}}{8}\mathcal{L}^{-1}\left\{\frac{1}{(s - s_1)(s - s_2)(s + i\mu)}\right\}(t) \\ \times\mathcal{L}^{-1}\left\{\frac{1}{(s - s_3)(s - s_4)(s - i\mu)}\right\}(t) \\ - \frac{\Gamma_N^2}{2}\mathcal{L}^{-1}\left\{\frac{s + i\varepsilon_{-\sigma} + \Gamma_N/2}{(s - s_1)(s - s_2)(s - i\mu)}\right\}(t) \\ \times\mathcal{L}^{-1}\left\{\frac{s - i\varepsilon_{-\sigma} + \Gamma_N/2}{(s - s_3)(s - s_4)(s + i\mu)}\right\}(t), \end{aligned} \tag{36}$$

where for $\sigma = \downarrow$ the replacement $(s_1, s_2) \rightarrow (s_3, s_3)$ should be made. Notice that for $\varepsilon_\uparrow = \varepsilon_\downarrow$ the conductance is spin independent ($G_\uparrow = G_\downarrow = G$).

In Fig. 8 we plot the time-dependent conductance $G_\sigma(\mu, t) = G$ as a function of μ for different phase difference between the superconducting leads, i.e., for $\phi = 0$ (upper panel) and for $\phi = 0.85\pi$ (bottom panel), in the presence of weakly coupled normal electrode, $\Gamma_N = 0.1\Gamma_S$ ($\Gamma_{S_1} = \Gamma_{S_2} = \Gamma_S = 1$) and $\varepsilon_\sigma = 0$. The process of forming the Andreev subgap states is clearly visible. We observe that for $\phi = 0$ in the limit of large time the conductance is characterized by two well pronounced maxima appearing at $\mu \simeq \pm\Gamma_S$ whose half-widths gradually shrink in time. These maxima appear after some time interval after abrupt switching of the QD-leads couplings (we denote such a time scale by τ_1, see Fig. 9). This characteristic time is needed to build up two distinct maxima of G and it depends on the phase difference ϕ—compare the upper and bottom panels in Fig. 8. Time evolution of such quasiparticle peaks allows us to estimate how fast the Andreev quasiparticles appear in the system, and thus it is desirable to study this process in more detail.

By inspecting $G_\sigma(\mu, t)$ in Fig. 8 we observe that up to some specific time τ_1, a broad one-peaked structure of G is present. Then, the conductance rapidly transforms in time into a two-peak structure. The position of each quasiparticle peak evolves in time to its steady limit value (that time is called τ_2) and finally the width and height of peaks are established after the time τ_f (see Fig. 9, bottom panel). In Fig. 9 we display the position of the quasiparticle peaks maxima vs time and μ for different values of Γ_N and ϕ indicated in the legend (upper panel). As one can see, the moment of the appearance of the two-peak structure, τ_1, depends on both ϕ and Γ_N. However, for $\phi = 0$ this time only slightly depends on Γ_N.

With increasing ϕ it increases with remarkable dependence on Γ_N (for a given ϕ it increases with Γ_N). The time scale for appearance of the two-peak structure is very small and for $\phi = 0$ it equals approximately 2.5 u.t., for $\phi = \pi/2$ it changes from $\sim$3 u.t. for $\Gamma_N = 0.1$ up to $\sim$4 u.t. for $\Gamma_N = 0.5$, and for $\phi = 3\pi/4$ it changes from $\sim$6 u.t. for $\Gamma_N = 0.1$ up to $\sim$8.5 u.t. for $\Gamma_N = 0.5$, respectively (see upper panel, Fig. 9). Positions of the maxima versus μ evolve in time during approximately $\tau_2 \simeq 12$ u.t. (the bold parts of lines in the bottom panel) and attain their steady-state values. Note that the asymptotic quasiparticle peaks heights and widths are achieved with the envelope function $1 - \exp(-t/\tau_f)$, where $\tau_f = \frac{2}{\Gamma_N}$ can be deduced from the explicit expression for $G_\sigma(\mu, t)$ in which the long living terms proportional to $\exp(-\Gamma_N t/2)$ are present.

Let us consider a few special cases, for which the simpler analytical formulas can be given. For $\phi = \pi$, $\varepsilon_\sigma = 0$, and $\Gamma_{S_1} = \Gamma_{S_2}$ the conductance takes the form (here $G_\uparrow = G_\downarrow = G$):

$$G(\mu, t) = \frac{\Gamma_N}{\left(\frac{\Gamma_N^2}{4} + \mu^2\right)}\left[\frac{\Gamma_N}{2} + e^{-\Gamma_N t/2}\cdot\left(\frac{\Gamma_N}{2}\cos(\mu t) - \Gamma_N \cosh\left(\frac{\Gamma_N t}{2}\right) + \mu \sin(\mu t)\right)\right]. \tag{37}$$

In this case the zero bias conductance reads $G(\mu = 0, t) = 2[1 + e^{-\Gamma_N t/2}(1 - 2\cosh(\Gamma_N t/2))]$ and for $t = 2\ln 2/\Gamma_N$ it reaches the optimal value equal to 0.5 and it vanishes for $t \to \infty$.

We notice the vanishing conductance $G_\sigma(\mu, t = \infty)$ for the symmetric couplings $\Gamma_{S_1} = \Gamma_{S_2}$ obtained for $\phi = \pi$. For $\Gamma_{S_1} \neq \Gamma_{S_2}$ the conductance is qualitatively different. Assuming $\frac{\Gamma_{S_2}}{\Gamma_{S_1}} = k$ we obtain $\Gamma_{12} = \Gamma_{S_1}^2(1 + k^2 + 2k\cos\phi)$, so for $k \neq 1$ and $\phi = \pi$ we get $\Gamma_{12} = \Gamma_{S_1}^2(1 - k)^2$. In such a case for calculating the conductance we should also take into account a contribution from the second term of Eq. (36). As differential conductance depends on the couplings Γ_{S_1}, Γ_{S_2}, and ϕ only through Γ_{12} therefore different choices of these parameters can lead to the same values of G_σ. The conductance calculated for $\Gamma_{S1} = \Gamma_{S2}$ and a given phase difference ϕ is identical to the one obtained for arbitrary asymmetric couplings $\Gamma_{S1}/\Gamma_{S2} = k$ using the effective phase difference $\bar{\phi} = \arccos((1 - k^2 + 2\cos\phi)/2k)$, where k satisfies the condition $|(1 - k^2 + 2\cos\phi)/2k| \leqslant 1$. It means that asymmetry in the couplings to superconducting leads Γ_{S_1}, Γ_{S_2} can be compensated by the phase difference parameter ϕ. This conclusion refers also to the QD occupancy and the current flowing between the QD and the normal lead. Since explicit expression for $G_\sigma(\mu, t)$ is rather lengthly, we skip it here and present only its asymptotic form ($t \to \infty$) for $\Gamma_{S_1} = \Gamma_{S_2} = \Gamma_S$, $\varepsilon_\uparrow = -\varepsilon_\downarrow$ ($G_\uparrow = G_\downarrow = G$)

$$G(\mu) = \frac{\Gamma_N^2\Gamma_S^2}{2}\cos^2\left(\frac{\phi}{2}\right)\left\{\frac{1}{\left(\frac{\Gamma_N^2}{4} + \mu_{-+}^2\right)\left(\frac{\Gamma_N^2}{4} + \mu_{++}^2\right)} + \frac{1}{\left(\frac{\Gamma_N^2}{4} + \mu_{+-}^2\right)\left(\frac{\Gamma_N^2}{4} + \mu_{--}^2\right)}\right\}, \tag{38}$$

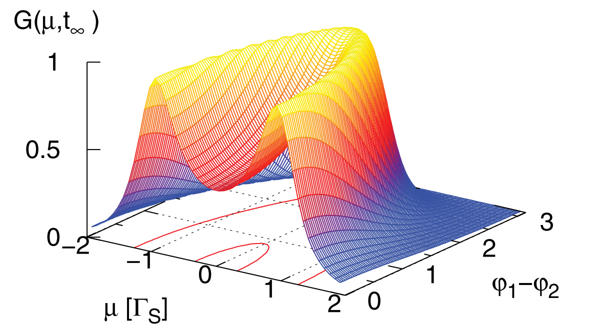

FIG. 10. The asymptotic conductance obtained for $t \to \infty$ as a function of μ and the phase difference $\phi = \varphi_1 - \varphi_2$. The contour lines correspond to $G = 0.5$ and $\Gamma_{S1} = \Gamma_{S2} = \Gamma_S$, $\Gamma_N = 0.75$.

where $\mu_{\alpha\beta} = \mu + E_{\alpha\beta}$. For $\Gamma_N \ll \Gamma_S$ the asymptotic conductance has four maxima placed at $\mu \simeq \pm\varepsilon_\uparrow \pm \Gamma_S|\cos(\frac{\phi}{2})|$ or equivalently at $\mu = E_{++}, E_{+-}, E_{-+}$ and E_{--}, respectively. Note that the asymptotic conductivity $G(\mu)$ does not depend on spin but in general $G_\sigma(\mu, t)$ can be spin dependent.

It is also interesting to check influence of the superconducting phase difference on the asymptotic Andreev conductance behavior. For arbitrary $\phi \neq \pi$ and $\varepsilon_\sigma = 0$, the asymptotic value of $G(\mu, t)$ can be written as follows (for $t = \infty$)

$$G(\mu) = \frac{\Gamma_N^2\Gamma_{12}}{4\left[\frac{\Gamma_N^2}{4} + \left(\frac{\sqrt{\Gamma_{12}}}{2} - \mu\right)^2\right]\left[\frac{\Gamma_N^2}{4} + \left(\frac{\sqrt{\Gamma_{12}}}{2} + \mu\right)^2\right]}. \tag{39}$$

Figure 10 presents the asymptotic conductance, $G(\mu, t = \infty)$, as a function of the bias voltage μ, and the phase difference ϕ. As one can see for $\phi = 0$ two distinct maxima of G are visible (cf. Fig. 8 for $t = 100$). For nonzero ϕ, which satisfies the condition $\cos(\phi) > \frac{\Gamma_N^2 - \Gamma_{S1}^2 - \Gamma_{S2}^2}{2\Gamma_{S1}\Gamma_{S2}}$, these two maxima appear at points $\mu = \pm\sqrt{\frac{\Gamma_{12}}{4} - \frac{\Gamma_N^2}{4}}$. In the opposite case, there is only one maximum at $\mu = 0$ whose height is reduced to zero value with $\phi \to \pi$. In consequence, for $\phi = \pi$ and $t = \infty$ the conductance vanishes for all μ. Note that for the QD coupled only to one superconducting and one normal electrode, the zero-bias conductance is invariant under the replacement $\Gamma_N \leftrightarrow \Gamma_S$, [70]. However, in our system with two superconducting leads this conclusion is no longer valid, even for the symmetric couplings case, $\Gamma_{S_1} = \Gamma_{S_2}$. Such a property is achieved only for $\phi = \frac{2\pi}{3}$.

In the last part of this section we discuss the time evolution of the ABS for nonzero splitting of the QD energy levels. In the first case we consider the symmetric splitting around the zero energy (Fig. 11, $\varepsilon_\uparrow = -\varepsilon_\downarrow = 0.5$ for $\phi = 0.85\pi$) and in the second case the splitting is symmetric but around the nonzero energy value equal 0.5 (Fig. 12, $\varepsilon_\uparrow = 1$, $\varepsilon_\downarrow = 0$ for some specific values of time after the quench). In Fig. 11 we analyze the approach to equilibrium of $G_\uparrow(\mu, t)$ for two values of Γ_N, $\Gamma_N = 0.1(0.02)$ upper (bottom) panel. We show only $G_\uparrow(\mu, t)$ as $G_\downarrow(\mu, t)$ is symmetric (with respect to $\mu = 0$) in relation to $G_\uparrow$. The maxima of $G_\uparrow$ for large time correspond to E_{-+}, E_{++}, E_{--}, and E_{+-} ABS states (beginning from negative values of the bias voltage μ). It is interesting that the time evolution of E_{-+}, E_{++} ABS is different from the evolution of E_{--} and E_{+-}, respectively. The stationary values of the conductance peaks corresponding to $G_\uparrow$ and $G_\downarrow$ are all

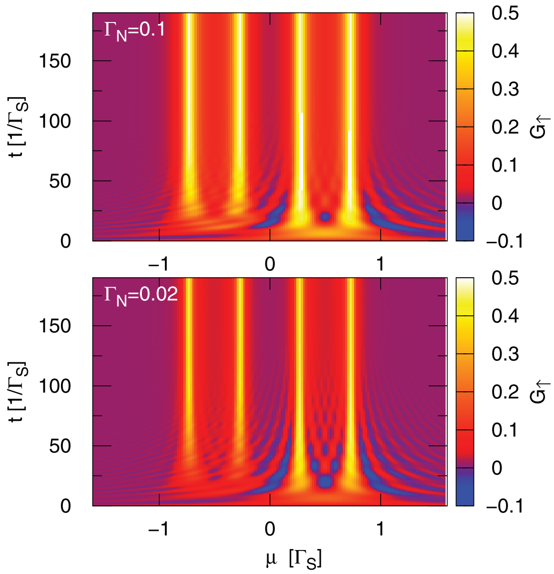

FIG. 11. Time-dependent Andreev conductance $G_\uparrow$ (in $4e^2/h$ units) as a function of the bias voltage μ for the phase difference $\phi = \varphi_1 - \varphi_2 = 0.85\pi$ and the Zeeman splitting $\varepsilon_\uparrow = -\varepsilon_\downarrow = 0.5$. The upper (bottom) panel corresponds to $\Gamma_N = 0.1$ ($\Gamma_N = 0.02$) and $\Gamma_{S1} = \Gamma_{S2} = \Gamma_S$.

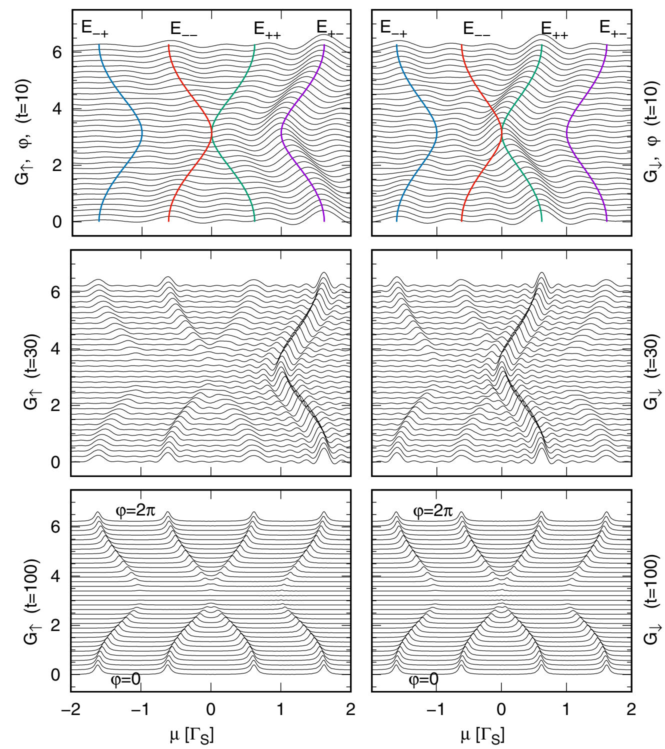

FIG. 12. Phase-dependent Andreev conductance $G_\uparrow$ (left panels) and $G_\downarrow$ (right panels) (in units of $4e^2/h$) as a function of the bias voltage μ for $t = 10$, 30, and 100 u.t. (upper, middle, and bottom panels, respectively) after the quench. Other parameters: $\varepsilon_\uparrow = 1$, $\varepsilon_\downarrow = 0$, $\Gamma_N = 0.1$, $\Gamma_{S1} = \Gamma_{S2} = \Gamma_S$. The lower curves in all panels correspond to $\phi = 0$ and each next upper curve is shifted up by $\frac{2\pi}{33}$, so the upper curves correspond to $\phi = 2\pi$. $E_{+-}, E_{++}, E_{--}, E_{-+}$ are represented by corresponding solid lines in the upper panels: They show the localization of the ABS (for $\Gamma_N = 0$) on the (μ, ϕ) plane.

the same [according to Eq. (38)] but the ABS E_{-+} and E_{++} begin to appear later than E_{--} and E_{+-}. For $\Gamma_N = 0.1$ (0.02) this delay time can be approximately estimated as 30 (60) u.t. For stronger coupling Γ_N (upper panel) the ABS peaks are wider in comparison to the case of weakly coupled normal electrode (bottom panel) and appear earlier than for smaller Γ_N.

In Fig. 12 we show the phase dependence of $G_\uparrow$ and $G_\downarrow$ calculated for small time, $t = 10$ u.t. (upper panels), for $t = 30$ u.t. (middle panels), and for long time, $t = 100$ u.t. (bottom panels) at which the conductance attains the stationary values. In addition, in the upper panels the curves representing the localization of the ABS states on the (μ, ϕ) plane are depicted. We observe the essential difference with strong asymmetry between $G_\uparrow$ and $G_\downarrow$ at a short period of time after the quench. The time evolution of $G_\uparrow$ ($G_\downarrow$) is limited to the appearance of E_{+-} (E_{++}) ABS. Next, for larger time other Andreev states appear but the most visible are still the curves corresponding to E_{+-} and E_{++}, respectively. Notice that for $\phi = \pi$ and large time the conductance vanishes for both spins [cf. Eq. (38)] as shown in the bottom panels. However, for smaller time after a quench the ABS states also vanish for $\phi = \pi$ except E_{+-} (for $\sigma = \uparrow$) and E_{++} (for $\sigma = \downarrow$). These states vanish only at relatively large times after the quench.

VII. CORRELATION EFFECTS

Finally let us address the correlation effects, driven by the Coulomb interactions $Uc_\uparrow^+ c_\uparrow c_\downarrow^+ c_\downarrow$ that should be added to the term H_{QD}. Such electrostatic repulsion is usually in conflict with the local electron pairing. In nanoscopic systems, however, their relationship is a bit more subtle. On one hand the Coulomb repulsion $U > 0$ suppresses the magnitude of on-dot pairing potential $\chi(t) = \langle c_\downarrow(t) c_\uparrow(t)\rangle$. In addition to this monotonous behavior, at some critical value U_c there occurs π shift of the complex function $\chi(t)$ [101]. Under such circumstances the subgap quasiparticles cross each other and the correlated quantum dot changes configuration of its ground state (singlet-doublet quantum phase transition). When the quantum dot is embedded into Josephson junction geometry, such an effect leads to reversal of dc supercurrent which has been extensively discussed by various groups [94,102].

Salient features of this π-shift effect can be captured within the lowest order perturbative treatment of the Coulomb term [101]. Crossing of the subgap quasiparticles can be qualitatively obtained using the Hartree-Fock-Bogoliubov decoupling scheme

$$c_\uparrow^+ c_\uparrow c_\downarrow^+ c_\downarrow \simeq n_\uparrow(t) c_\downarrow^+ c_\downarrow + n_\downarrow(t) c_\uparrow^+ c_\uparrow - n_\uparrow(t) n_\downarrow(t) + \chi^*(t) c_\uparrow^+ c_\downarrow^+ + \chi(t) c_\downarrow c_\uparrow - |\chi(t)|^2. \tag{40}$$

In this mean-field treatment we can absorb the Hartree-Fock terms to the renormalized QD energy level $\epsilon_\sigma + U n_{-\sigma}(t)$ and the anomalous (pair source/sink) terms rescale the effective on-dot pairing to $\frac{1}{2}(\Gamma_{S_1} e^{i\varphi_1} + \Gamma_{S_2} e^{i\varphi_2}) - U\chi(t)$. In a weak coupling regime $U < U_c$ the lowest order approximation (40)

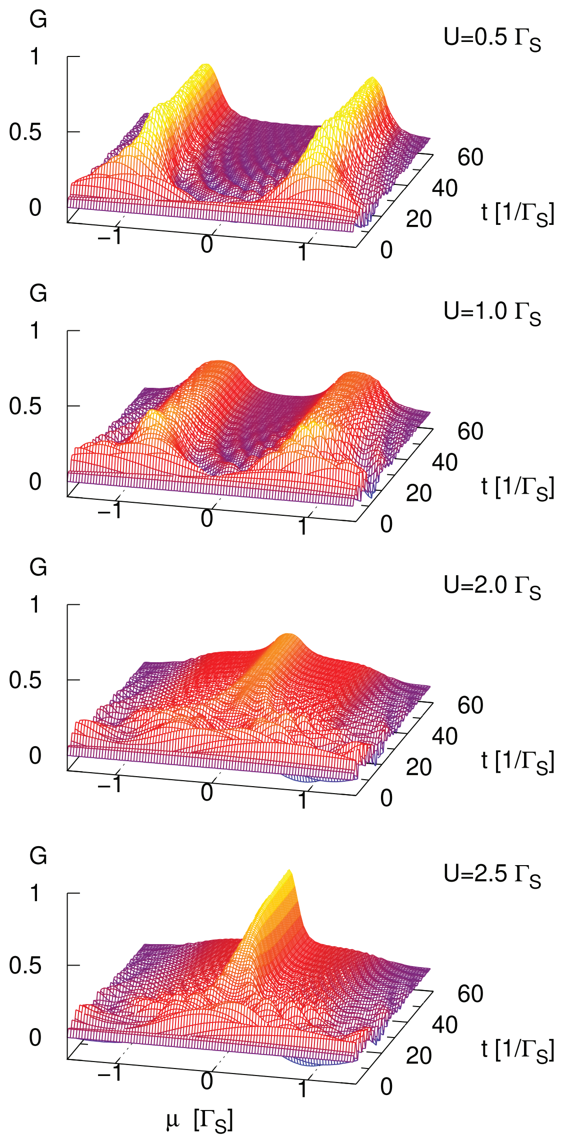

FIG. 13. Time-dependent differential conductance $G \equiv G_\sigma$ (expressed in units of $4e^2/h$) as a function the bias voltage μ obtained for the correlated quantum dot, assuming $\epsilon = -U/2$ and several values of U as indicated. The phase difference is $\varphi_1 - \varphi_2 = 0$ and $\Gamma_N = 0.1\Gamma_S$. We assumed the initial QD occupancy $n_\sigma(t=0) = 0$.

has been shown to qualitatively reproduce the results of more sophisticated many-body techniques [92,101].

Since analytical determination of the time-dependent observables is no longer possible, we have investigated the correlation effects by means of self-consistent numerical calculations. In what follows, we focus on the special case $\varepsilon_\sigma = -U/2$ which in the stationary limit corresponds to the half-filled quantum dot $n_\sigma(t \to \infty) = \frac{1}{2}$. We have computed the time-dependent occupancy $n_\sigma(t)$ and the complex pairing potential $\chi(t)$, solving the differential equations of motion for the relevant expectation values [80] by the Runge-Kutta algorithm.

In Fig. 13 we show representative results, which illustrate time-dependent buildup of the subgap quasiparticles of the correlated quantum dot. In analogy to the discussion in Sec. VI (corresponding to the noninteracting case), we present the differential Andreev conductance $G(\mu)$ versus the bias voltage μ obtained numerically for $\varphi_1 = \varphi_2$ and several values of the Coulomb potential U, as indicated. Comparison with the top panel of Fig. 8 clearly indicates that the subgap quasiparticle peaks gradually move closer towards each other upon increasing the Coulomb potential U. At the critical value $U_c \simeq 2\Gamma_S$, they finally merge into the single (rather broad) peak, signaling the mentioned $0-\pi$ transition. In the strongly correlated regime ($U > U_c$) this structure should split again into two separate peaks, but unfortunately the Hartree-Fock-Bogolubov approximation (40) fails to properly account for such physical effect. We are predominantly interested in the transient phenomena, therefore description of the strong correlations (including realization of the subgap Kondo effect) is beyond a scope of the present analysis.

By inspecting the panels of Fig. 13 we notice that frequency of the transient oscillations depends on the potential U. This is a rather obvious fact, considering that Coulomb repulsion has direct influence on the energies of subgap quasiparticles [93]. Furthermore, electron correlations seem to substantially enlarge a temporal region of the quasiparticle buildup (characterized by the time scale τ_f). For a more reliable study of this nontrivial interplay between the transient and correlation effects there should be used some sophisticated (nonperturbative) methods.

VIII. SUMMARY

We have investigated the dynamics of subgap quasiparticles for the setup comprising the quantum dot (QD) embedded between two superconducting leads and another metallic electrode. Transient phenomena, caused by an abrupt coupling of the QD to external reservoirs, have been studied solving the Heisenberg equations of motion within the Laplace transform technique which easily incorporates the initial conditions. We have determined the time-dependent charge and magnetization of QD, development of the on-dot pairing, and transient currents induced under the equilibrium (for identical chemical potentials of the leads) and nonequilibrium conditions (i.e., for the biased system). Similar effects can be also observed in the Josephson junctions periodically driven by external fields [103].

In the limit of large energy gap of superconducting reservoirs we have derived analytical formulas for time-dependent observables. We have distinguished between two contributions appearing in expressions for the QD occupancy $n_\sigma(t)$, on-dot pairing amplitude $\langle c_\downarrow(t) c_\uparrow(t)\rangle$, and charge current flowing between the QD and superconducting leads. The first term depends on the initial QD occupancy (but is not dependent on the chemical potentials of external reservoirs) and is responsible for an oscillating transient behavior of the considered quantities, with a characteristic damping $\exp(-\Gamma_N t)$ driven by the QD-normal lead coupling Γ_N. Contribution of this term is proportional to the factor $(1 - n_\uparrow(0) - n_\downarrow(0))$, so it can vanish for some specific initial QD occupancies $n_\sigma(0)$. The second part appearing in the considered formulas depends mainly on Γ_N and it induces a monotonous time dependence of the observables. The latter term is present in all expressions, regardless of the initial conditions.

We have studied dependence of the amplitude and the period of transient oscillations on the model parameters. We have shown that under specific initial conditions (assuming either the empty and doubly-occupied initial QD configurations) these oscillations are reminiscent of Rabi-type transitions, typical for a two-level system, which in our case correspond to a pair of the Andreev states.

We have also checked influence of the phase difference ϕ between superconducting reservoirs on transient phenomena. For $\varepsilon_\sigma = 0$ the asymptotic occupancy of QD seems to be independent on such phase difference. However, in the presence of the Zeeman splitting the occupancies $n_\sigma(t)$ become sensitive to ϕ and reveal an abrupt change of the QD magnetization $n_\uparrow(t) - n_\downarrow(t)$. Right after the quench this feature is obscured by transient phenomena, however, it becomes more and more evident starting from $t \geqslant \frac{4}{\Gamma_N}$ (Fig. 3). Finally, we have analyzed the time-dependent differential conductance of the charge current induced by the bias voltage applied to the normal lead. Its phase dependence exhibits the two-peak structure (typical for the stationary limit) which gradually develops within a finite time interval. This characteristic time scale increases with respect to the phase difference ϕ and can be spin dependent in the presence of the Zeeman splitting. Unexpectedly, we have found a puzzling particle-hole asymmetric development of the subgap quasiparticles, which ultimately become symmetric and spin independent in the asymptotic limit $t \to \infty$.

Since transient currents are measurable by the present-day experimental resolution in the subpicosecond regime, we hope that such spectroscopy could precisely determine all time scales, characteristic for the subgap quasiparticles of the proximitized quantum dots. They could be also extended onto heterostructures with topological superconductors, probing the dynamical properties of more exotic Majorana-type quasiparticles.

ACKNOWLEDGMENTS

This work was supported by National Science Centre (NCN, Poland) under Grant No. UMO-2017/27/B/ST3/01911 (T.D. and R.T.).

[1] A.-P. Jauho, N. S. Wingreen, and Y. Meir, Time-dependent transport in interacting and noninteracting resonant-tunneling systems, Phys. Rev. B **50**, 5528 (1994).

[2] Q.-F. Sun and T.-H. Lin, Transient current through a quantum dot with two time-dependent barriers, J. Phys.: Condens. Matter **9**, 3043 (1997).

[3] P. Nordlander, M. Pustilnik, Y. Meir, N. S. Wingreen, and D. C. Langreth, How Long Does it Take for the Kondo Effect to Develop?, Phys. Rev. Lett. **83**, 808 (1999).

[4] T. Fujisawa, D. G. Austing, Y. Tokura, Y. Hirayama, and S. Tarucha, Electrical pulse measurement, inelastic relaxation, and nonequilibrium transport in a quantum dot, J. Phys.: Condens. Matter **15**, R1395 (2003).

[5] Y. Zhu, J. Maciejko, T. Ji, H. Guo, and J. Wang, Time-dependent quantum transport: Direct analysis in the time domain, Phys. Rev. B **71**, 075317 (2005).

[6] M. Plihal, D. C. Langreth, and P. Nordlander, Transient currents and universal time scales for a fully time-dependent quantum dot in the Kondo regime, Phys. Rev. B **71**, 165321 (2005).

[7] A. F. Izmaylov, A. Goker, B. A. Friedman, and P. Nordlander, Transient current in a quantum dot subject to a change in coupling to its leads, J. Phys.: Condens. Matter **18**, 8995 (2006).

[8] J. Maciejko, J. Wang, and H. Guo, Time-dependent quantum transport far from equilibrium: An exact nonlinear response theory, Phys. Rev. B **74**, 085324 (2006).

[9] F. M. Souza, Spin-dependent ringing and beats in a quantum dot system, Phys. Rev. B **76**, 205315 (2007).

[10] V. Moldoveanu, V. Gudmundsson, and A. Manolescu, Transient regime in nonlinear transport through many-level quantum dots, Phys. Rev. B **76**, 085330 (2007).

[11] A. Goker, B. A. Friedman, and P. Nordlander, Transient current in a quantum dot asymmetrically coupled to metallic leads, J. Phys.: Cond. Matter **19**, 376206 (2007).

[12] Z. Feng, J. Maciejko, J. Wang, and H. Guo, Current fluctuations in the transient regime: An exact formulation for mesoscopic systems, Phys. Rev. B **77**, 075302 (2008).

[13] T. L. Schmidt, P. Werner, L. Mühlbacher, and A. Komnik, Transient dynamics of the Anderson impurity model out of equilibrium, Phys. Rev. B **78**, 235110 (2008).

[14] E. Perfetto, G. Stefanucci, and M. Cini, Spin-flip scattering in time-dependent transport through a quantum dot: Enhanced spin-current and inverse tunneling magnetoresistance, Phys. Rev. B **78**, 155301 (2008).

[15] G. Stefanucci, E. Perfetto, and M. Cini, Ultrafast manipulation of electron spins in a double quantum dot device: A real-time numerical and analytical study, Phys. Rev. B **78**, 075425 (2008).

[16] V. Moldoveanu, A. Manolescu, and V. Gudmundsson, Geometrical effects and signal delay in time-dependent transport at the nanoscale, New J. Phys. **11**, 073019 (2009).

[17] V. Gudmundsson, C. Gainar, C.-S. Tang, V. Moldoveanu, and A. Manolescu, Time-dependent transport via the generalized master equation through a finite quantum wire with an embedded subsystem, New J. Phys. **11**, 113007 (2009).

[18] V. Moldoveanu, A. Manolescu, and V. Gudmundsson, Theoretical investigation of modulated currents in open nanostructures, Phys. Rev. B **80**, 205325 (2009).

[19] T. L. Schmidt and A. Komnik, Charge transfer statistics of a molecular quantum dot with a vibrational degree of freedom, Phys. Rev. B **80**, 041307(R) (2009).

[20] H. Pan and Y. Zhao, Time-dependent quantum transport behavior through T-shaped double quantum dots, J. Phys.: Condens. Matter **21**, 265501 (2009).

[21] Y. Tomita, T. Nakayama, and H. Ishii, Transient current behavior through molecular bridge systems; effects of intra-molecule current on quantum relaxation and oscillation, e-J. Surf. Sci. and Nanotechnology **7**, 606 (2009).

[22] P. Myöhänen, A. Stan, G. Stefanucci, and R. van Leeuwen, Kadanoff-Baym approach to quantum transport through interacting nanoscale systems: From the transient to the steady-state regime, Phys. Rev. B **80**, 115107 (2009).
[23] A. Croy and U. Saalmann, Propagation scheme for nonequilibrium dynamics of electron transport in nanoscale devices, Phys. Rev. B **80**, 245311 (2009).
[24] Q.-F. Sun, J. Wang, and T.-H. Lin, Photon-assisted Andreev tunneling through a mesoscopic hybrid system, Phys. Rev. B **59**, 13126 (1999).
[25] V. Moldoveanu, A. Manolescu, C.-S. Tang, and V. Gudmundsson, Coulomb interaction and transient charging of excited states in open nanosystems, Phys. Rev. B **81**, 155442 (2010).
[26] J. Jin, M. W.-Y. Tu, W.-M. Zhang, and Y. J. Yan, Non-equilibrium quantum theory for nanodevices based on the Feynman-Vernon influence functional, New J. Phys. **12**, 083013 (2010).
[27] Ph. Werner, T. Oka, M. Eckstein, and A. J. Millis, Weak-coupling quantum Monte Carlo calculations on the Keldysh contour: Theory and application to the current-voltage characteristics of the anderson model, Phys. Rev. B **81**, 035108 (2010).
[28] A. Komnik, Transient dynamics of the nonequilibrium majorana resonant level model, Phys. Rev. B **79**, 245102 (2009).
[29] B. Wang, Y. Xing, L. Zhang, and J. Wang, Transient dynamics of molecular devices under a steplike pulse bias, Phys. Rev. B **81**, 121103(R) (2010).
[30] E. C. Cuansing and J.-S. Wang, Transient behavior of heat transport in a thermal switch, Phys. Rev. B **81**, 052302 (2010).
[31] S.-H. Ke1, R. Liu, W. Yang, and H. U. Baranger, Time-dependent transport through molecular junctions, J. Chem. Phys. **132**, 234105 (2010).
[32] P. Myöhänen, A. Stan, G. Stefanucci, and R. van Leeuwen, Kadanoff-Baym approach to time-dependent quantum transport in AC and DC fields, J. Phys.: Confer. Series **220**, 012017 (2010).
[33] H. D. Cornean, C. Gianesello, and V. Zagrebnov, A partition-free approach to transient and steady-state charge currents, J. Phys. A: Math. and Theor. **43**, 474011 (2010).
[34] S. Andergassen, M. Pletyukhov, D. Schuricht, H. Schoeller, and L. Borda, Renormalization group analysis of the interacting resonant-level model at finite bias: Generic analytic study of static properties and quench dynamics, Phys. Rev. B **83**, 205103 (2011).
[35] D. Segal, A. Millis, and D. Reichman, Nonequilibrium transport in quantum impurity models: exact path integral simulations, Phys. Chem. Chem. Phys. **13**, 14378 (2011).
[36] A. Croy, U. Saalmann, A. R. Hernández, and C. H. Lewenkopf, Nonadiabatic electron pumping through interacting quantum dots, Phys. Rev. B **85**, 035309 (2012).
[37] K. Joho, S. Maier, and A. Komnik, Transient noise spectra in resonant tunneling setups: Exactly solvable models, Phys. Rev. B **86**, 155304 (2012).
[38] E. Taranko, M. Wiertel, and R. Taranko, Transient electron transport properties of multiple quantum dots systems, J. Appl. Phys. **111**, 023711 (2012).
[39] E. Khosravi, A.-M. Uimonen, A. Stan, G. Stefanucci, S. Kurth, R. van Leeuwen, and E. K. U. Gross, Correlation effects in bistability at the nanoscale: Steady state and beyond, Phys. Rev. B **85**, 075103 (2012).
[40] G. Stefanucci and C.-O. Almbladh, Time-dependent partition-free approach in resonant tunneling systems, Phys. Rev. B **69**, 195318 (2004).
[41] L. D. Contreras-Pulido, J. Splettstoesser, M. Governale, J. König, and M. Büttiker, Time scales in the dynamics of an interacting quantum dot, Phys. Rev. B **85**, 075301 (2012).
[42] L. Zhang, Y. Xing, and J. Wang, First-principles investigation of transient dynamics of molecular devices, Phys. Rev. B **86**, 155438 (2012).
[43] D. M. Kennes, S. G. Jakobs, C. Karrasch, and V. Meden, Renormalization group approach to time-dependent transport through correlated quantum dots, Phys. Rev. B **85**, 085113 (2012).
[44] W. Pei, X. C. Xie, and Q. f. Sun, Transient heat generation in a quantum dot under a step-like pulse bias, J. Phys.: Condens. Matter **24**, 415302 (2012).
[45] L. Zhang, J. Chen, and J. Wang, First-principles investigation of transient current in molecular devices by using complex absorbing potentials, Phys. Rev. B **87**, 205401 (2013).
[46] M. Kulkarni, K. Tiwari, and D. Segal, Full density matrix dynamics for large quantum systems: interactions, decoherence and inelastic effects, New J. Phys. **15**, 013014 (2013).
[47] K. F. Albrecht, A. Martín-Rodero, R. C. Monreal, L. Mühlbacher, and A. Levy Yeyati, Long transient dynamics in the Anderson-Holstein model out of equilibrium, Phys. Rev. B **87**, 085127 (2013).
[48] I. Knezevic and B. Novakovic, Time-dependent transport in open systems based on quantum master equations, J. Comput. Electron. **12**, 363 (2013).
[49] R. Tuovinen, R. van Leeuwen, E. Perfetto, and G. Stefanucci, Time-dependent Landauer-Buttiker formula for transient dynamics, J. Phys.: Confer. Series **427**, 012014 (2013).
[50] R. Taranko and P. Parafiniuk, Influence of the Coulomb interaction on the spin-polarized current in the quantum dot system in the presence of the bias voltage pulse, Physica E **49**, 5 (2013).
[51] T. Kwapiński and R. Taranko, Charging time effects and transient current beats in horizontal and vertical quantum dot systems, Physica E **63**, 241 (2014).
[52] V. Vovchenko, D. Anchishkin, J. Azema, P. Lombardo, R. Hayn, and A.-M. Dare, A new approach to time-dependent transport through an interacting quantum dot within the Keldysh formalism, J. Phys.: Condens. Matter **26**, 015306 (2014).
[53] R. Tuovinen, E. Perfetto, G. Stefanucci, and R. van Leeuwen, Time-dependent Landauer-Büttiker formula: Application to transient dynamics in graphene nanoribbons, Phys. Rev. B **89**, 085131 (2014).
[54] G.-M. Tang and J. Wang, Full-counting statistics of charge and spin transport in the transient regime: A nonequilibrium Green's function approach, Phys. Rev. B **90**, 195422 (2014).
[55] G.-M. Tang, F. Xu, and J. Wang, Waiting time distribution of quantum electronic transport in the transient regime, Phys. Rev. B **89**, 205310 (2014).
[56] R. Seoane Souto, R. Avriller, R. C. Monreal, A. Martín-Rodero, and A. Levy Yeyati, Transient dynamics and waiting time distribution of molecular junctions in the polaronic regime, Phys. Rev. B **92**, 125435 (2015).

[57] R. Taranko and T. Kwapiński, Charge and current beats in T-shaped qubit-detector systems, Physica E **70**, 217 (2015).
[58] B. Dong, G. H. Ding, and X. L. Lei, Time-dependent quantum transport through an interacting quantum dot beyond sequential tunneling: second-order quantum rate equations, J. Phys.: Condens. Matter **27**, 205303 (2015).
[59] R. Tuovinen, N. Säkkinen, D. Karlsson, G. Stefanucci, and R. van Leeuwen, Phononic heat transport in the transient regime: An analytic solution, Phys. Rev. B **93**, 214301 (2016).
[60] M. M. Odashima and C. H. Lewenkopf, Time-dependent resonant tunneling transport: Keldysh and Kadanoff-Baym nonequilibrium Green's functions in an analytically soluble problem, Phys. Rev. B **95**, 104301 (2017).
[61] M. Ridley, A. MacKinnon, and L. Kantorovich, Partition-free theory of time-dependent current correlations in nanojunctions in response to an arbitrary time-dependent bias, Phys. Rev. B **95**, 165440 (2017).
[62] R. Seoane Souto, A. Martín-Rodero, and A. Levy Yeyati, Analysis of universality in transient dynamics of coherent electronic transport, Fortschritte der Physik **65**, 1600062 (2017).
[63] X. Chen, J. Yuan, G. Tang, J. Wang, Z. Zhang, C.-M. Hu, and H. Guo, Transient spin current under a thermal switch, J. Phys. D: Appl. Phys. **51**, 274004 (2018).
[64] G. Tang, Z. Yu, and J. Wang, Full-counting statistics of energy transport of molecular junctions in the polaronic regime, New J. Phys. **19**, 083007 (2017).
[65] H.-T. Chen, G. Cohen, A. J. Millis, and D. R. Reichman, Anderson-Holstein model in two flavors of the noncrossing approximation, Phys. Rev. B **93**, 174309 (2016).
[66] R. Seoane Souto, A. Martín-Rodero, and A. Levy Yeyati, Quench dynamics in superconducting nanojunctions: Metastability and dynamical Yang-Lee zeros, Phys. Rev. B **96**, 165444 (2017).
[67] P.-Y. Yang, C.-Y. Lin, and W.-M. Zhang, Master equation approach to transient quantum transport in nanostructures incorporating initial correlations, Phys. Rev. B **92**, 165403 (2015).
[68] Y. Xing, Q.-F. Sun, and J. Wang, Response time of a normal-metal/superconductor hybrid system under a step-like pulse bias, Phys. Rev. B **75**, 125308 (2007).
[69] M. Governale, M. G. Pala, and J. König, Real-time diagrammatic approach to transport through interacting quantum dots with normal and superconducting leads, Phys. Rev. B **77**, 134513 (2008).
[70] T. Domański and A. Donabidowicz, Interplay between particle-hole splitting and the Kondo effect in quantum dots, Phys. Rev. B **78**, 073105 (2008).
[71] K. F. Albrecht, H. Soller, L. Muhlbacher, and A. Komnik, Transient dynamics and steady state behavior of the Anderson-Holstein model with a superconducting lead, Physica E **54**, 15 (2013).
[72] A. Koga, Quantum Monte Carlo study of nonequilibrium transport through a quantum dot coupled to normal and superconducting leads, Phys. Rev. B **87**, 115409 (2013).
[73] L. Rajabi, C. Pöltl, and M. Governale, Waiting Time Distributions for the Transport through a Quantum-Dot Tunnel Coupled to One Normal and One Superconducting Lead, Phys. Rev. Lett. **111**, 067002 (2013).
[74] E. Perfetto, G. Stefanucci, and M. Cini, Equilibrium and time-dependent Josephson current in one-dimensional superconducting junctions, Phys. Rev. B **80**, 205408 (2009).
[75] G. Stefanucci, E. Perfetto, and M. Cini, Time-dependent quantum transport with superconducting leads: A discrete-basis Kohn-Sham formulation and propagation scheme, Phys. Rev. B **81**, 115446 (2010).
[76] R. Seoane Souto, A. Martín-Rodero, and A. Levy Yeyati, Andreev Bound States Formation and Quasiparticle Trapping in Quench Dynamics Revealed by Time-Dependent Counting Statistics, Phys. Rev. Lett. **117**, 267701 (2016).
[77] G. Michałek, B. R. Bułka, T. Domański, and K. I. Wysokiński, Statistics of tunneling events in three-terminal hybrid devices with quantum dot, Acta Phys. Polon. A **133**, 391 (2018).
[78] R. Seoane Souto, R. Avriller, A. Levy Yeyati, and A. Martín-Rodero, Transient dynamics in interacting nanojunctions within self-consistent perturbation theory, New J. Phys. **20**, 083039 (2018).
[79] S. Mi, P. Burset, and Ch. Flindt, Electron waiting times in hybrid junctions with topological superconductors, Sci. Rep. **8**, 16828 (2018).
[80] R. Taranko and T. Domański, Buildup and transient oscillations of Andreev quasiparticles, Phys. Rev. B **98**, 075420 (2018).
[81] G. Stefanucci and R. van Leeuwen, *Nonequilibrium Manybody Theory of Quantum Systems: A Modern Introduction* (Cambridge Univeristy Press, 2013).
[82] A. Eichler, M. Weiss, S. Oberholzer, C. Schönenberger, A. Levy Yeyati, J. C. Cuevas, and A. Martín-Rodero, Even-Odd Effect in Andreev Transport Through a Carbon Nanotube Quantum Dot, Phys. Rev. Lett. **99**, 126602 (2007).
[83] R. S. Deacon, Y. Tanaka, A. Oiwa, R. Sakano, K. Yoshida, K. Shibata, K. Hirakawa, and S. Tarucha, Tunneling Spectroscopy of Andreev Energy Levels in a Quantum Dot Coupled to a Superconductor, Phys. Rev. Lett. **104**, 076805 (2010).
[84] J.-D. Pillet, P. Joyez, R. Žitko, and M. F. Goffman, Tunneling spectroscopy of a single quantum dot coupled to a superconductor: From Kondo ridge to Andreev bound states, Phys. Rev. B **88**, 045101 (2013).
[85] F. M. Souza, S. A. Leão, R. M. Gester, and A. P. Jauho, Transient charging and discharging of spin-polarized electrons in a quantum dot, Phys. Rev. B **76**, 125318 (2007).
[86] R. Maurand, T. Meng, E. Bonet, S. Florens, L. Marty, and W. Wernsdorfer, First-Order $0-\pi$ Quantum Phase Transition in the Kondo Regime of a Superconducting Carbon-Nanotube Quantum Dot, Phys. Rev. X **2**, 011009 (2012).
[87] R. Delagrange, D. J. Luitz, R. Weil, A. Kasumov, V. Meden, H. Bouchiat, and R. Deblock, Manipulating the magnetic state of a carbon nanotube Josephson junction using the superconducting phase, Phys. Rev. B **91**, 241401(R) (2015).
[88] R. Delagrange, R. Weil, A. Kasumov, M. Ferrier, H. Bouchiat, and R. Deblock, 0-π quantum transition in a carbon nanotube Josephson junction: Universal phase dependence and orbital degeneracy, Phys. Rev. B **93**, 195437 (2016).
[89] T. Jonckheere, A. Zazunov, K. V. Bayandin, V. Shumeiko, and T. Martin, Nonequilibrium supercurrent through a quantum dot: Current harmonics and proximity effect due to a normal-metal lead, Phys. Rev. B **80**, 184510 (2009).
[90] A. Oguri, Y. Tanaka, and J. Bauer, Interplay between Kondo and Andreev-Josephson effects in a quantum dot coupled to

one normal and two superconducting leads, Phys. Rev. B **87**, 075432 (2013).

[91] G. Kiršanskas, M. Goldstein, K. Flensberg, L. I. Glazman, and J. Paaske, Yu-Shiba-Rusinov states in phase-biased superconductor–quantum dot–superconductor junctions, Phys. Rev. B **92**, 235422 (2015).

[92] T. Domański, M. Žonda, V. Pokorný, G. Górski, V. Janiš, and T. Novotný, Josephson-phase-controlled interplay between correlation effects and electron pairing in a three-terminal nanostructure, Phys. Rev. B **95**, 045104 (2017).

[93] J. Bauer, A. Oguri, and A. C. Hewson, Spectral properties of locally correlated electrons in a Bardeen-Cooper-Schrieffer superconductor, J. Phys.: Cond. Matter **19**, 486211 (2007).

[94] A. Martín-Rodero and A. Levy Yeyati, Josephson and Andreev transport through quantum dots, Adv. Phys. **60**, 899 (2011).

[95] Y. Yamada, Y. Tanaka, and N. Kawakami, Interplay of Kondo and superconducting correlations in the nonequilibrium Andreev transport through a quantum dot, Phys. Rev. B **84**, 075484 (2011).

[96] D. Futterer, J. Świebodziński, M. Governale, and J. König, Renormalization effects in interacting quantum dots coupled to superconducting leads, Phys. Rev. B **87**, 014509 (2013).

[97] I. Weymann and P. Trocha, Superconducting proximity effect and zero-bias anomaly in transport through quantum dots weakly attached to ferromagnetic leads, Phys. Rev. B **89**, 115305 (2014).

[98] G. Schaller, Ph. Zedler, and T. Brandes, Systematic perturbation theory for dynamical coarse-graining, Phys. Rev. A **79**, 032110 (2009).

[99] C. Cohen-Tannoudji, B. Diu, and F. Laloe, *Quantum Mechanics* (A Wiley-Interscience Publications, Paris, 1977), Vol. 1.

[100] K. I. Wysokiński, Thermoelectric transport in the three terminal quantum dot, J. Phys.: Cond. Matter **24**, 335303 (2012).

[101] M. Žonda, V. Pokorný, V. Janiš, and T Novotný, Perturbation theory of a superconducting 0 - π impurity quantum phase transition, Sci. Rep. **5**, 8821 (2015).

[102] V. Meden, The Anderson-Josephson quantum dot – A theory perspective, J. Phys.: Cond. Matter **31**, 163001 (2019).

[103] N. W. Hendrickx, M. L. V. Tagliaferri, M. Kouwenhoven, R. Li, D. P. Franke, A. Sammak, A. Brinkman, G. Scappucci, and M. Veldhorst, Ballistic supercurrent discretization and micrometer-long Josephson coupling in germanium, Phys. Rev. B **99**, 075435 (2019).